Domein Formation Mechanisms of Block and Graft Copolymers from Their Solutions

AUTHOR(S):

KAWAI, Hiromichi; SOEN, Toshiichi; INOUE, Takashi; ONO, Takashi; UCHIDA, Takanori

CITATION:

KAWAI, Hiromichi ...[et al]. Domein Formation Mechanisms of Block and Graft Copolymers from Their Solutions. Memoirs of the Faculty of Engineering, Kyoto University 1972, 33(4): 383-445

ISSUE DATE:

1972-03-31

URL:

http://hdl.handle.net/2433/280868

Domain Formation Mechanisms of Block and Graft Copolymers from Their Solutions

By

Hiromichi KAWAI,* Toshiichi SOEN,* Takashi INOUE,**
Takashi ONO,+ and Takanori UCHIDA++

(Received June 30, 1971)

I. Introduction

Since the proposal by Merrett in 1954 of "organic lattices" stabilized by the interactions between homo-polymeric subchains of block or graft copolymers and selective solvents,[1,2] this concept of micelle formation has been extended, as comprehensivly reviewed by Molau,[3] not only for understanding the domain formation mechanisms of the copolymers from their solutions in either selective or non-selective solvents, but also for explaining the "polymeric oil-in-oil" emulsifying effects of the copolymers upon the domain formations of mixtures of the corresponding homo-polymers from their solutions in the non-selective solvents.

It has been suggested by Sadron[4,5] and Vanzo[6] that the two-phase structure of block copolymers in the solid state is influenced by the configurations of the polymer chains, micro-phase separation of the block segments, at a critical concentration during the solvent casting process. On the other hand, Molau *et al.*[7-9], Riess *et al.*[10], and Kohler *et al.*[11], have carried out experimental studies on the emulsifying effects of the block and graft copolymers, which restrain the phase separation of the mixed system of the corresponding homo-polymers into their macroscopic domains and keep the system micro-heterogeneous.

* Department of Polymer Chemistry
** Present address: Research Center, Japan Synthetic Rubber Co., Ltd., Mochiisaka, Ikuta, Kawasaki, Kanagawa-ken, Japan.
+ Present address: Non-metallic Materials Division, Toyota Motors Co., Ltd., Toyota, Aichi-ken, Japan.
++ Present address: Market Research Laboratory, Mitsubishi Chemical Industries Ltd., Hisamoto-Kamoi-cho, Kawasaki, Kanagawa-ken, Japan.

In contrast to the rather numerous studies on the domain formation mechanism of block copolymers, the studies on graft copolymers have been relatively few. Actually, although the concept of organic lattices of Merrett arose originally from the fractionation of the primary products during the grafting of vinyl polymers onto natural rubber,[1] only a few studies on graft copolymers speculating about the micelle formation in solutions and the subsequent domain structures in solid state from their solution properties and bulk properties, respectively, have appeared in the literature.[12-17] On the other hand, the emulsifying effects of graft copolymers have been considerably studied in connection with the polymerization of a solution of one polymer in a monomer of a different type,[7-9] because this method of preparing polymeric oil-in-oil emulsions has commercial significance, playing an important role in the formation of certain rubber-modified plastics, such as high-impact polystyrene and ABS resins.[18,19]

Recent developments in anionic polymerization technique[20,21] have made it possible to synthesize graft copolymers as well as several types of block copolymers, such as A-B, A-B-A, and B-A-B type block copolymers, which have very definite molecular structures and, in addition, are relatively free in the choice of the types of A and B segments. In other words, the developments have made it possible for us to study the domain formation mechanisms of block and graft copolymers not only for understanding the concepts of "organic lattices" as well as "polymeric oil-in-oil emulsions" in a more quantitative manner, but also for establishing a technology for good control of the domain structures of a heterogeneous system of, at least, two polymer components, in terms of the size and shape of the domains and the molecular architecture within the domains as well.

In this article, studies on the domain formation mechanisms of block and graft copolymers, which have been mostly carried out by the present authors at the Department of Polymer Chemistry, Kyoto University, from 1966 to 1970, will be reviewed. That is, the domain formation mechanism of an A-B type block copolymer of styrene and isoprene from its solutions will be first discussed in terms of the thermodynamic and molecular parameters, *i.e.*, the free energy of micelle formation at the critical micelle concentration during the solvent casting process.[22,23] Then, the domain structures of solvent-cast films of several compositions of three component systems, the A-B type block copolymer of styrene and isoprene, homo-polystyrene, and homo-polyisoprene, will be further discussed qualitatively in terms of the thermodynamic parameters of phase equilibria in the four component system, including the solvent,

by taking account of the inherent nature of the domain formation of the A-B type block copolymer, the concept of formation of organic lattices, and the emulsifying effects of the block copolymer, as well.[24]

Furthermore, the domain formation mechanisms of multi-block copolymers, such as A-B-A and B-A-B type block copolymers, from their solutions will be discussed in terms of the further modifications of the thermodynamic and molecular parameters obtained for the A-B type block copolymer.[25] The experimental data obtained, not only by the present authors for the A-B-A type block copolymer of styrene-isoprene-styrene, but also by Matsuo *et al.*[26] for the A-B-A and B-A-B type block copolymers of styrene-butadiene-styrene and butadiene-styrene-butadiene, respectively, will be utilized.[27] Finally, the domain formation mechanism of a graft copolymer of poly (methyl acrylate) with styrene, obtained by grafting polystyryllithium onto a well-fractionated poly (methyl acrylate), will be discussed in comparison with the domain formation mechanism of block copolymers.[28]

II. Domain Formation Mechanism of an A-B Type Block Copolymer of Styrene and Isoprene From Its Solutions[22,23]

A. Experimental Procedures and Results

1. Preparation of A-B Type Block Copolymers of Styrene and Isoprene

A-B type block copolymers of styrene and isoprene were synthesized by an anionic polymerization technique, a "living polymerization" technique using *n*-BuLi as an initiator, varying the fractions of the A and B block segments from zero to unity. The selection of styrene and isoprene for the A and B segments was based on the following reason: polystyrene is guite incompatible with polyisoprene, which makes the phase separation of the system very definite; both monomers have been well-studied with respect to anionic polymerization; the difference in the glass-transition temperatures between the two components is large enough to characterize the bulk properties of the system in terms of the domain structures; and, in addition, polyisoprene is selectively stained by OsO_4 due to its diene structure, which not only makes the ultrathin sectioning of cast specimens for electron microscopic observation of the domain structure easy, but also gives very clear results because of the deep contrast of the selective staining of the isoprene component.[29]

Isoprene and styrene monomers, as well as tetrahydrofuran (THF), the polymerization solvent, were carefully purified by the method of Morton *et al.*[30-32] and collected under a vacuum (10^{-6} mmHg) in separate ampoules equipped with magnetic breakseals. Polymerization of the styrene monomer, and

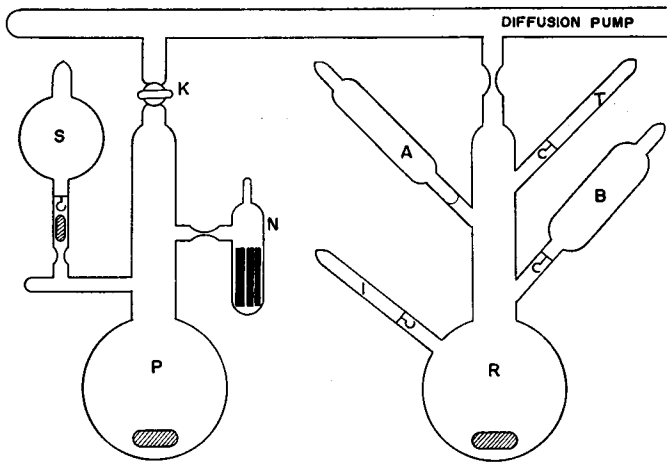

Fig. 1. Schematic representation of block copolymerization apparatus: (S) polymerization solvent (THF); (P) purification flask for the solvent; (N) sodium lumps; (R) polymerization flask; (I) polymerization initiator for styrene (*n*-BuLi solution in *n*-hexane); (A) styrene monomer; (B) isoprene monomer; (T) polymerization terminator (*n*-BuOH solution in THF).

then of the isoprene monomer, was performed in a block copolymerization apparatus connected to a vacuum line, as shown schematically in Fig. 1. The THF solvent was further purified by means of the Na mirror technique in flask P and flash-distilled to flask R through stopcock K and the main vacuum line L. The polymerization of styrene was then effected by mixing the initiator solution (*n*-BuLi solution in *n*-hexane) I and the styrene monomer A in THF at dry ice-methanol temperature. The reaction, which gave a reddish yellow color, was allowed to continue until the monomer was completely consumed. Then, block copolymerization of isoprene to the polystyrene block sequence was carried out by adding the isoprene monomer B to the solution containing (living) polystyryllithium anion as the initiator. The reaction, which gave a yellow solution, was terminated by adding *n*-butanol solution in THF after about 20 hr.

2. *Characterization of Block Copolymers*

The block copolymers thus obtained were characterized by velocity ultracentrifugation, osmotic pressure, and ultraviolet and infrared spectroscopy.

Sedimentation Pattern. The sedimentation pattern of a 0.5 g/l THF solution of the copolymer (observed at 20°C in a Spinco Model E ultracentrifuge at 59,780 rpm) exhibited a very sharp single peak as shown in Fig. 2 a. This behavior was observed in all the copolymers used in the experiments. In con-

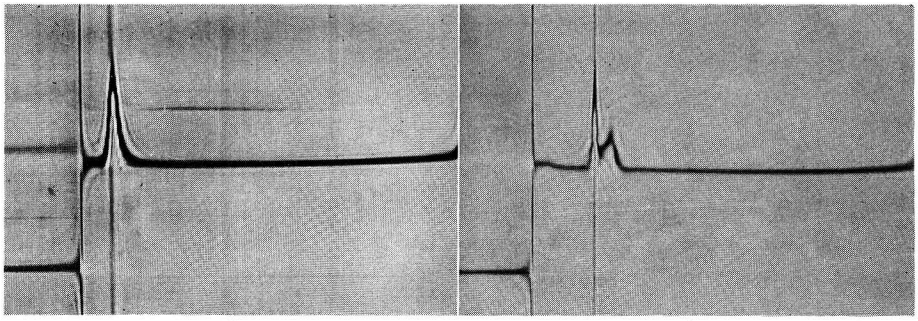

(a) (b)

Fig. 2. Sedimentation pattern from Spince Model E ultractrifuge: (a) 0.5 g/*l*. THF solution of a 40/60 styrene-isoprene block copolymer at 59,780 rpm, (20°C, 24 min; Schlieren angle 75°); (b) 0.5 g/*l*. THF solution of a block copolymer contaminated by homo-polystyrene at 56,100 rpm, (20°C, 28 min; Schlieren angle 75°).

trast, Fig. 2 b demonstrates a twin peak sedimentation pattern for a copolymer containing some homo-polystyrene. The homo-polystyrene was produced from impurities in the isoprene monomer, which destroyed some of the polystyryllithium anions. In addition to the sedimentation pattern, the fact that the color of living anions changed from reddish yellow to yellow during the block copolymerization suggest that the polymers used for the experiment were genuine A-B type block copolymers uncontaminated by the homo-polymers of styrene and isoprene.

Molecular Weight. The number-averaged molecular weights, as determined in a toluene solution at 37.0°C with a high-speed membrane osmometer, are listed in Table 1, together with specimen codes of the respective block copolymers.

Table 1. Characterization of A-B Type Block Copolymers of Styrene-Isoprene Used.

Specimen code	$\bar{M}_n \times 10^{-4}$*	Wt fraction of styrene, %**	Optical appearance of film cast from toluene
SI-1 (20/80 Sty-Isop)	27.8	18	Transparent but very slightly iridescent.
SI-2 (40/60 Sty-Isop)	53.8	43	Transparent but iridescent.
SI-3 (50/50 Sty-Isop)	70.1	49	Slightly cloudy and iridescent.
SI-4 (60/40 Sty-Isop)	22.1	—	Transparent but slightly iridescent.
SI-5 (70/30 Sty-Isop)	104	73	Transparent but iridescent.

* Measured by a high speed membrane osmometer in toluene solution at 37°C.

** Determined from UV absorption at 262 mμ in CCl_4 solution.

Fraction of A-B Block Sequences. The weight fraction of the styrene blocks was determined in CCl_4 solution (at a polymer concentration of ca. 0.2 g/l) from the ultraviolet absorption at 262 mμ, a characteristic absorption band for polystyrene.[33] These results are also listed in Table 1.

Infrared Spectrum. To judge from the infrared absorption spectrum from 810 to 930 cm^{-1} (which will be illustrated later in connection with dichroic characterization), the isoprene appears mostly as the 3, 4 and 1, 2 addition polymer; *trans*-1, 4 addition takes place to a small extent.[34]

The copolymers thus prepared were cast into films about 0.2 mm thick by pouring relatively dilute solutions of 1 % to 10 % concentrations in various solvents onto a glass plate floating on mercury and evaporating the solvents very gradually at about 20°C. The film specimens thus formed were further dried under a vacuum of about 10^{-4} mmHg for a few days.

3. *Electron Microscopy*

The domain structure of the film specimens thus prepared was investigated with an electron microscopy using the osmium tetroxide fixation technique developed by Kato.[29] Ultrathin sections of about 350 Å thickness were cut normal to the films surfaces by an LKB ultramicrotome. The dark portions in the micrographs are definitely the polyisoprene phase, which is selectively stained by OsO_4 because of the unsaturated component in this phase.

Change of Domain Structure with Fraction of Block Sequences. For specimens cast from a 5 % toluene solution, the domain formation of the two-phase structure originating from the microphase separation of the block segments was observed. As can be seen in Fig. 3, the domain structure changed in a systematic manner with increasing fractions of the styrene sequence. The junctions between the polystyrene and polyisoprene segments in each block chain should be distributed along the boundary between the two phases.

The domain structure of a 20/80 styrene-isoprene block copolymer (SI-1, Fig. 3 a) may be characterized as tiny spheres of styrene component dispersed in a matrix of isoprene component. On the othet hand, the structures of 40/60 and 50/50 styrene-isoprene block copolymers (SI-2 and SI-3, Figs. 3 b and 3 c) are characterized as zebra patterns of alternating stripes of each component, where for the 40/60 copolymer the isoprene phase is somewhat dominant owing to the slightly greater isoprene fraction.

It has been clarified stereographically, as illustrated in Fig. 4, that the alternating stripe pattern is a sectional view of an alternating lamellar arrangement of the two components, *i. e.*, each component separates into lamellae oriented parallel to the film surface.[22] The iridescent color effect, which has

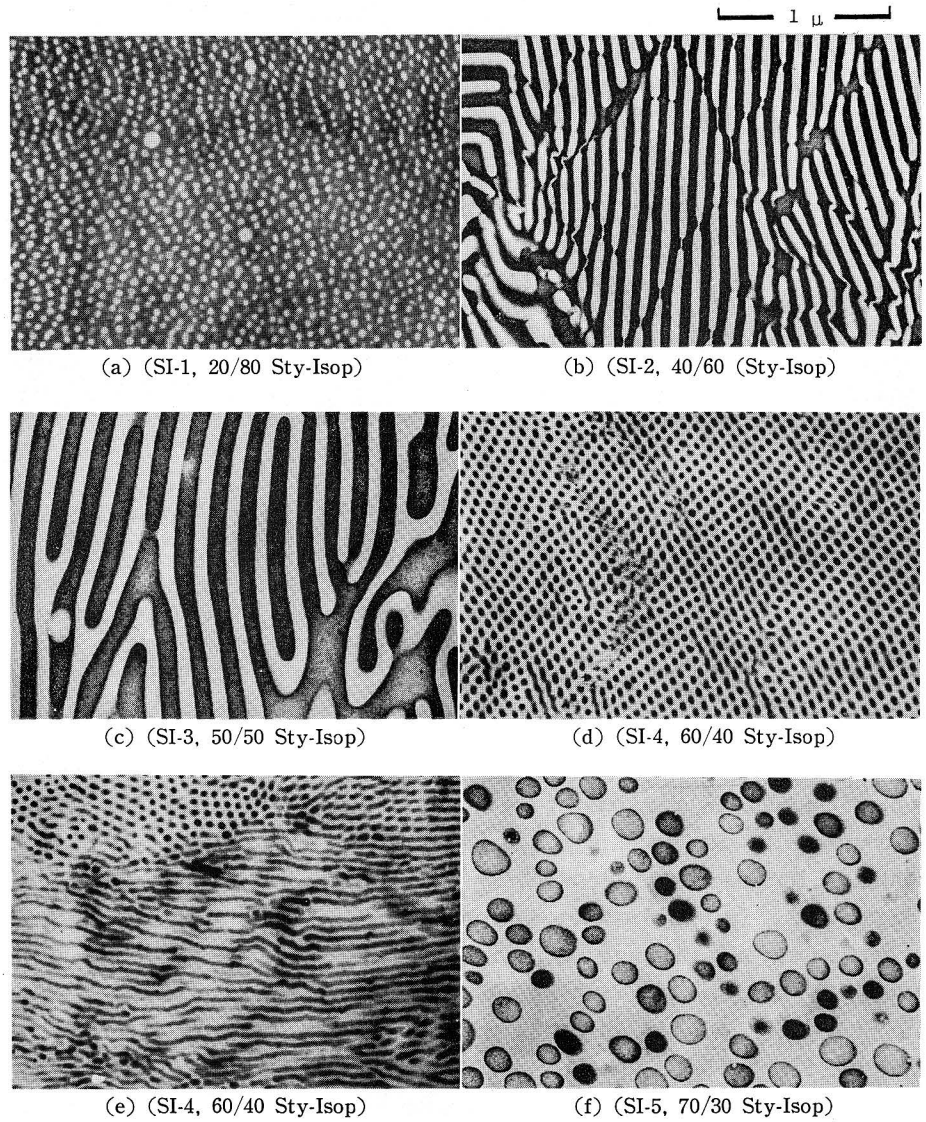

(a) (SI-1, 20/80 Sty-Isop) (b) (SI-2, 40/60 (Sty-Isop)

(c) (SI-3, 50/50 Sty-Isop) (d) (SI-4, 60/40 Sty-Isop)

(e) (SI-4, 60/40 Sty-Isop) (f) (SI-5, 70/30 Sty-Isop)

Fig. 3. Electron micrographs of ultrathin sections (*ca.* 350Å thick) cut normal to the surfaces of films cast from 5 % toluene solutions of styrene-isoprene block copolymers varying in composition from 20 % to 70 % (wt) fractions of styrene.

been already pointed out by Vanzo and ascribed to the periodic nature of the structure,[6] was also observed, especially for the 40/60 and 50/50 copolymers, in the solid as well as in the swollen polymer when the concentration was greater than a critical concentration of about 10 %.

The domain structures of a 60/40 styrene-isoprene block copolymer (SI-4,

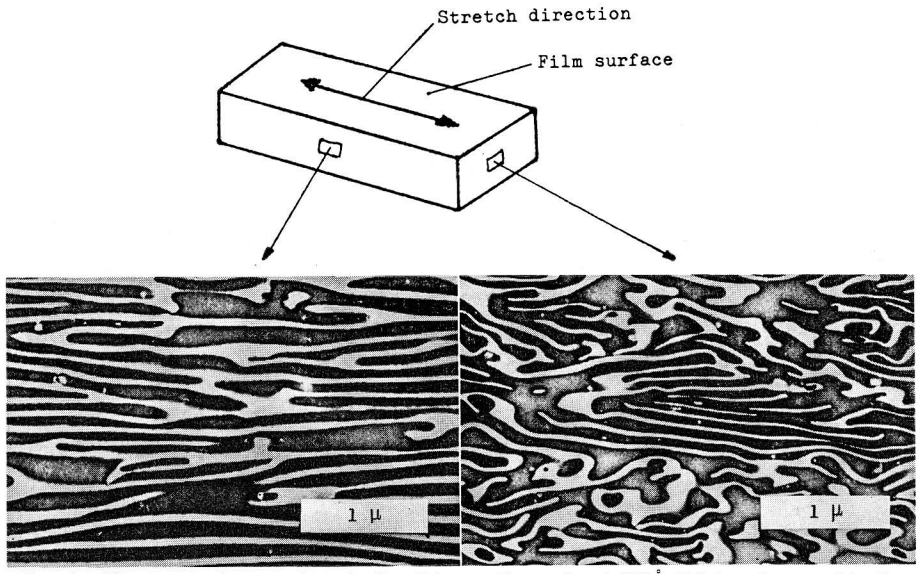

Fig. 4. Electron micrographs of ultrathin sections about 350Å thick cut normal to the surface of a film cast from about 5 % toluene solution of a styrene-isoprene block copolymer (SI-3, 50/50 Sty-Isop) and stretched by 100 % elongation at 130°C. Left, parallel to the stretching direction; right, perpendicular to the stretching direction.

Fig. 3 d) may be characterized, like those of the 20/80 copolymer, as spheres of one component in a matrix of the other component, but the roles of the two components are exchanged. However, the arrangement of the spherical domains of the isoprene component is much more regular than that of the 20/80 copolymer in Fig. 3 a, and, as can be recognized from Fig. 3 e, an ultrathin section cut also normal but in a different direction from that in Fig. 3 d, in which rod-like domains rather than the spherical domains of the isoprene component can partly be seen, the very regular arrangement of the spherical domains in Fig. 3 d is an apparent sectional view of rod-like domains oriented very parallel not only to each other but also to the film surface.

The domain structure of a 70/30 styrene-isoprene block copolymer (SI-5, Fig. 3 f) may be characterized as spheres of isoprene component dispersed in a matrix of styrene component. As can be seen, however, in Fig. 3 f, some spherical domains are quite darkened, whereas the other domains are darkened only at their boundaries to the matrix. But, when one restains the ultrathin section with OsO_4, every spherical domain becomes quite dark. This suggests that OsO_4, diffusing through the matrix, deposits on the surface of the spherical domain of the isoprene component and reduces to metallic osmium, preventing

further diffusion into the spherical domain, resulting in a dark circular pattern as the surface view and an open circular pattern as the cross-sectional view of the spherical domain of isoprene component.

According to the terminology used by one of the present authors for classifying heterogeneous mixtures of two incompatible components,[34] the above systematic change of the domain structure with an increasing fraction of styrene proceeds from an A-islands-in-B-matrix morphology, to either an A-matrix-B-matrix or an A-islands-B-islands form, and thence to a B-islands-in-A-matrix form.

Change of Domain Structure with Casting Solvent. In order to investigate the effect of casting solvent on the domain structure, a 40/60 block copolymer was cast from solutions of about 2.5 % concentration in various solvents at room temperature. Electron microscopic textures obtained by the OsO_4 fixation technique are illustrated in Fig. 5.

The domain structure of the 40/60 block copolymer cast from methyl ethyl ketone (MEK) (Fig. 5 b), cyclohexane (Fig. 5 c), carbon tetrachloride (Fig. 5 d), *n*-hexane (Fig. 5 e), and *iso*-octane (Fig. 5 f) may be classified, in general, as polystyrene-islands-in-polyisoprene-matrix in contrast to the alternating lamellar arrangement observed in Fig. 5 a for toluene casting, irrespective of the somewhat lower concentration of the casting solution than that in Fig. 3 b.

The spape and size of the polystyrene islands are different from one solvent to another, which probably reflects differences in solvation power for the block segments of the copolymer. It is difficult, however, to demonstrate a systematic change of the domain structure with solvation because of the lack of exact knowledge of this parameter, except for the quantitative representation in terms of the solubility parameters, such as Small has proposed.[35]

The domain structures cast from MEK, carbon tetrachloride, and cyclohexane seem to be more irregular than the alternating lamellar structure obtained from the toluene solution. Of these solvents, MEK may be classified as a good solvent for styrene segments but a poor solvent for isoprene segments; carbon tetrachloride and cyclohexane are just the opposite, whereas toluene is a rather good solvent for both segments.

The electron micrograph of a film specimen cast from cyclohexane (Fig. 5 c) reveals only two kinds of patterns of the unstained styrene component; *i. e.*, circular patterns almost identical in diameter and parallel stripes of various length and almost the same width as the diameters of the circles, being in contrast to the more irregular patterns of the other specimens. This suggests that the electron micrograph should be understood as a sectonal view

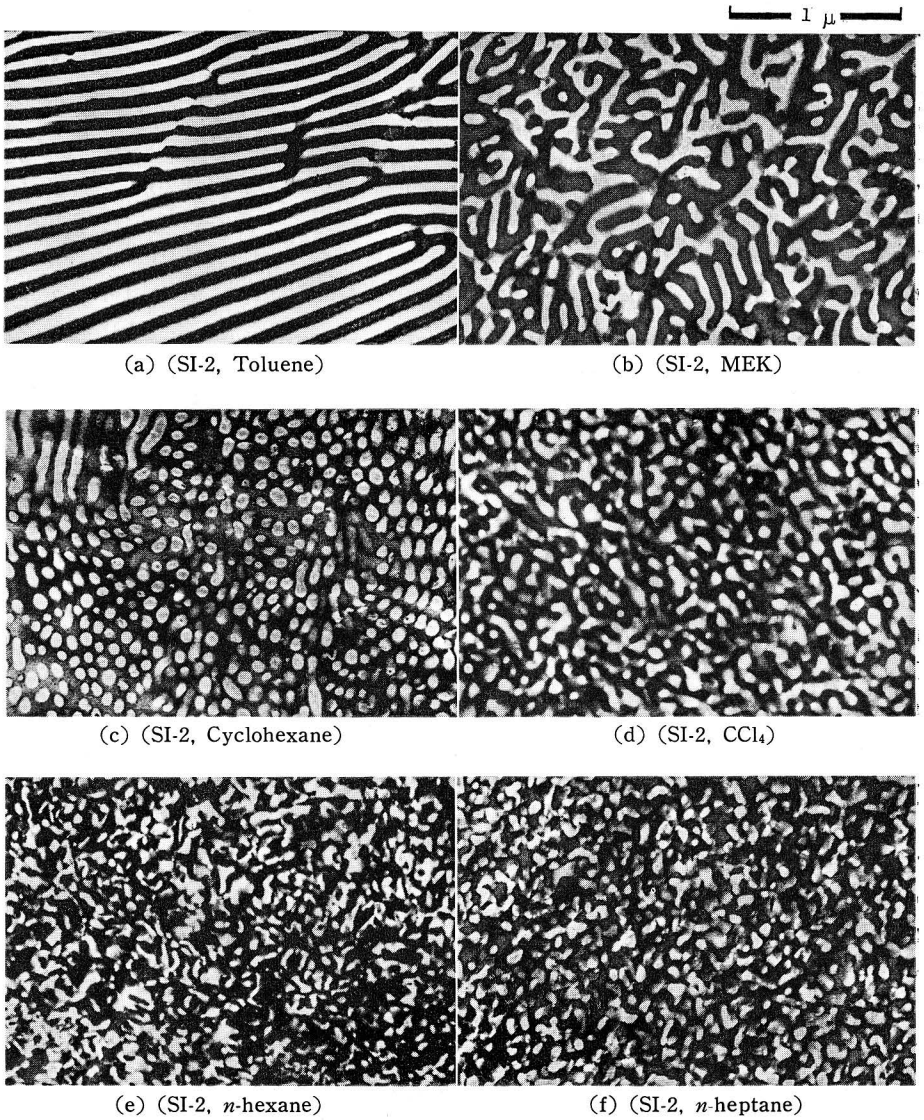

(a) (SI-2, Toluene) (b) (SI-2, MEK)

(c) (SI-2, Cyclohexane) (d) (SI-2, CCl_4)

(e) (SI-2, *n*-hexane) (f) (SI-2, *n*-heptane)

Fig. 5. Electron micrographs of ultrathin sections (*ca.* 350Å thick) cut normal to the surfaces of films cast from 2.5 % solutions of a styrene-isoprene blook copolymer (SI-2 40/60 Sty-Isop) in various solvents.

of almost identical rods of styrene component arranged nearly parallel in a matrix of isoprene component. This domain structure of styrene rods dispersed in a matrix of isoprene component must be emphasized in contrast to the domain structure of the 60/40 block copolymer in Fig. 3 d, which is just the opposite in the roles of the two components.

The domain structures observed in Fig. 5 c, as well as in Fig. 3 d, rod-like domains of one component dispersed in a matrix of the other component, should be considered as one of the simplest but most fundamental structures, together with the structures of spherical domains of one component in a matrix of the other component and the alternating lamellar arrangement of the two components. The existence of the rodlike domain structure has also been clearly demonstrated by Matsuo,[26] as will be discussed later.

The structures cast from *n*-hexane and *iso*-octane are composed of much smaller and more irregular fragments of the styrene component dispersed in the isoprene matrix than those obtained from the other solvents. Both *n*-hexane and *iso*-octane are good solvents for the isoprene segments but extremely poor solvents or nonsolvents for the styrene segments. The solutions are actually milky white and must be regarded as pseudo-solutions in which the precipitated polystyrene chains are kept in suspension by the block segments of polyisoprene which are so well solvated and expanded in the solvent as to give the

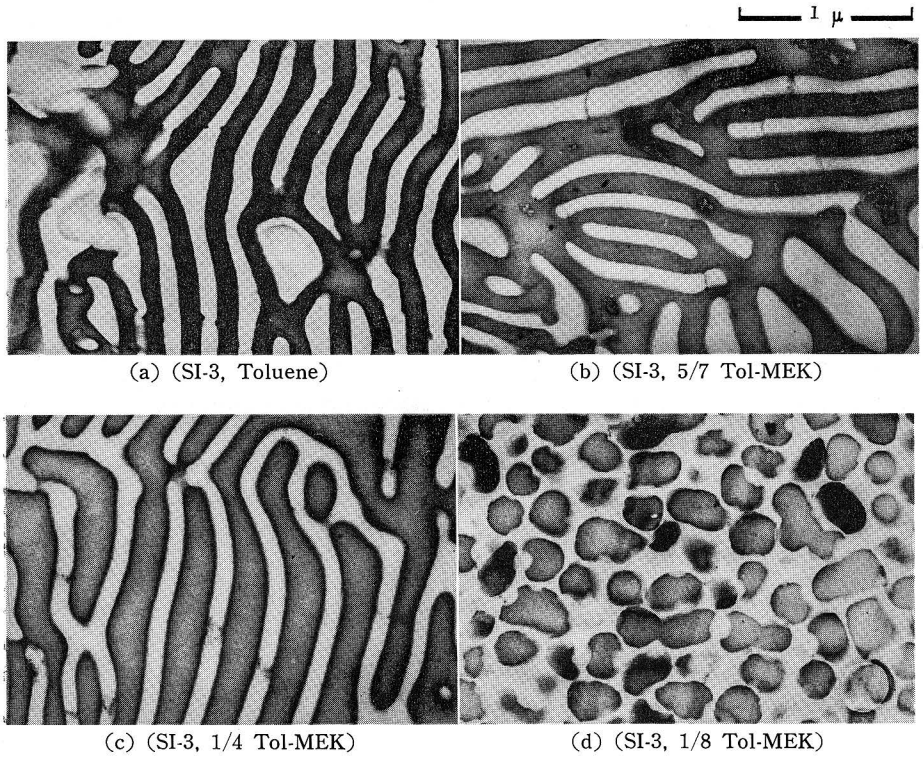

(a) (SI-3, Toluene) (b) (SI-3, 5/7 Tol-MEK)

(c) (SI-3, 1/4 Tol-MEK) (d) (SI-3, 1/8 Tol-MEK)

Fig. 6. Electron micrographs of ultrathin sections (*ca.* 350Å thick) cut normal to the surfaces of films cast from 5 % solutions of a styrene-isoprene block copolymer (SI-3, 50/50 Sty-Isop) in mixed solvents of toluene with MEK in various fractions.

above-mentioned structure of the isoprene matrix.

Fig. 6 demonstrates also the change of domain structure with casting solvent, using the 50/50 block copolymer (SI-3) and mixed solvents of toluene with MEK in various fractions. As seen in the figure, with increasing fractions of MEK, a good solvent for the styrene segments but a poor solvent for the isoprene segments, the original domain structure cast from toluene solution to give an alternating lamellar arrangement changes to one greatly dominant in the styrene component, and eventually to spherical domains of isoprene component in a matrix of styrene component.

Effect of Initial Concentration of Solution upon Domain Structure. In order to check the effect of the initial polymer concentration in the casting solution on the domain structure formed in the film specimen, the 40/60 block copolymer (SI-2) was cast from toluene solution at room temperature over a wide range of initial concentrations below a critical concentration (a little higher than 10 %), the criterion being the appearance of an iridescent color.

Fig. 7 illustrates two extreme results for a 0.8 % solution (Fig. 7 a) and a 10 % solution (Fig. 7 b), which give essentially the same structure, the alternating lamellar arrangement of both components, as illustrated in Fig. 3 b from 5 % solution and in Fig. 5 a from 2.5 % solution. This suggests that the domain structure is unaffected if the initial concentration is kept below the critical concentration.

Actually, iridescence appeared for all solutions tested when evaporation during casting brought the concentration to its critical value, a little higher than 10 % in this system. Thus, it appears that the domain structure originates as an equilibrium phenomenon at the critical concentration irrerpective

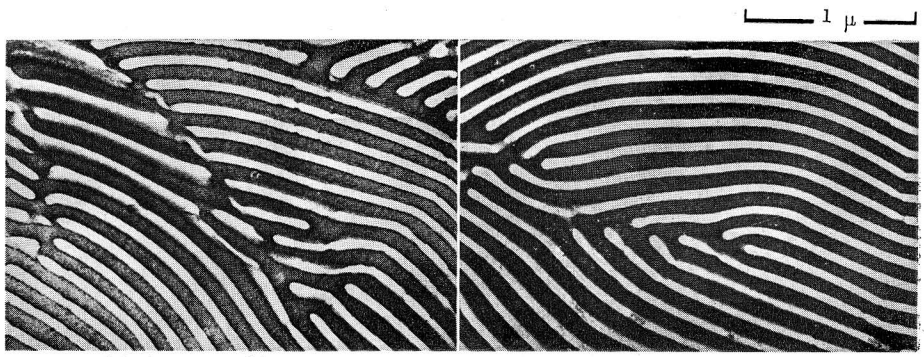

(a) (SI-2, 0.8 % toluene) (b) (SI-2, 10 % toluene)

Fig. 7. Electron micrographs of ultrathin sections (*ca.* 350Å thick) cut normal to the surfaces of films of a styrene-isoprene block copolymer (SI-2, 40/60 Sty-Isop) cast from toluene solutions differing in initial polymer concentration.

of the initial concentration and is carried over into the solid state.

B. Fundamental Domain Structure and Molecular Orientation

As has been shown in the previous sections, the two-phase structures of the A-B block copolymers cast from solutions may be represented by the following three types of fundamental domain structures: (a) spheres of one component dispersed in a matrix of the other component, (b) rods of one component, almost parallel, dispersed in a matrix of the other component, and (c) an alternating lamellar arrangement of the two components.

When the A-B block copolymer chains are organized into these fundamental domain structures, all of the junction points of the block chains must be arranged at the interface between the two phases. The respective domain structures and the molecular arrangements within the domains are illustrated schematically in the upper half of Fig. 8.

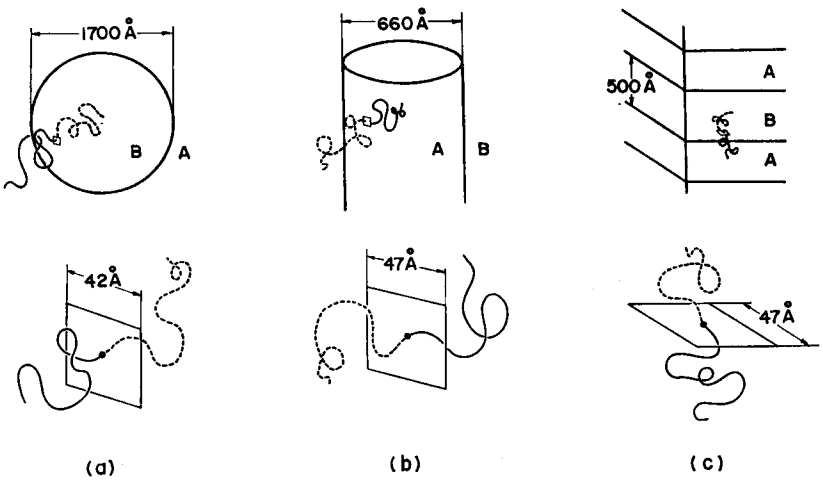

Fig. 8. Schematic representations of three types of fundamental domain structure, molecular orientations within the domains, and effectively occupied area per chain block in the interface between the two separate components: (a) spheres of one component (isoprene) dispersed in a matrix of the other component (styrene); (b) rods of one component (styrene) in a matrix of the other component (isoprene); (c) alternating lamellar arrangement of the two components. These correspond to Figs. 3f, 5c, and 3c, respectively.

By assuming that the density of each component within the domain structure is identical with that of each homo-polymer in bulk, *i.e.*, $\rho_{sty}=1.052$ and $\rho_{isop}=0.925$, the effectively occupied area per chain block at the interface may be evaluated from the average dimensions of the domains and the average degrees of polymerization of the block segments. The occupied areas per chain

block thus evaluated for each kind of domain structure are illustrated in the lower half of Fig. 8, together with the dimensions of each domain evaluated from the respective electron micrographs as average values.[22] It is noted that the calculated areas are all close to 1600 Å^2. When these calculated areas are compared with the dimensions of the respective domains, it becomes apparent that the block chains must be stretched and oriented along the direction perpendicular to the interface; *i.e.*, radial direction for the spherical and rod-like domains and normal to the lamellar surface for the alternating lamellar domains.

This has been confirmed experimentally by means of polarized infrared dichroism studies of film specimens of the 40/60 and 50/50 block copolymers cast from toluene solutions, which give, as previously demonstrated, alternating lamellar structures oriented parallel to the film surface. Some parallel dichroism of the 880, 909, and 1493 cm^{-1} absorption bands with respect to the direction normal to the film surface was observed, as illustrated in Fig. 9, with polarized infrared radiation directed to the tilted film surface at an angle of 30° from the film normal. The film specimens were unfortunately too thick to give a clear difference between the polarized radiations with electric vectors parallel and perpendicular to the plane including the incident ray and the film normal. However, small but definite differences observed for each band

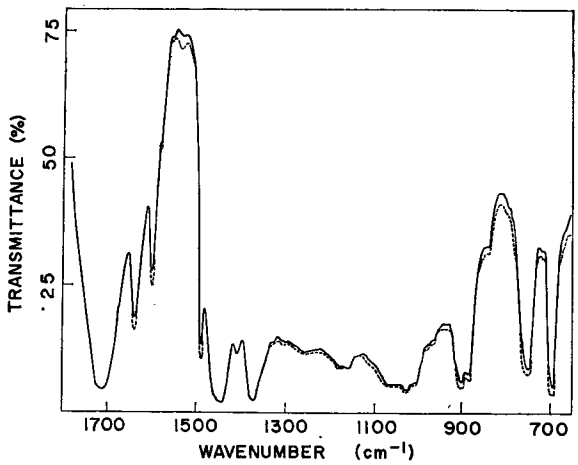

Fig. 9. Infrared spectra of a thin film of styrene-isoprene block copolymer (SI-3, 50/50 Sty-Isop) cast from toluene solution; polarized infrared radiation incident at an angle of 30° to the normal to the film surface. (——) Radiation polarized parallel and (------) radiation polarized perpendicular to the plane including the incident ray and the filmn ormal.

at a relatively low transmittance level may be enough to suggest a fairly large dichroism for the bands when the tilting angle is taken into consideration.

The parallel dichroism of the 889 and 909 cm^{-1} bands suggests that the polyisoprene segments are preferentially oriented perpendicular to the film surface,[36] *i.e.*, perpendicular to the lamellar plane. However, the parallel dichroism of the 1493 cm^{-1} styrene band does not necessarily suggest preferential orientation of polystyrene segments along the lamellar plane. The net transition moment, which arises from the $\nu_{19A}(A_1)$ benzene mode of the C-C bond between the benzene ring and the main chain,[37] is strongly dependent on the conformation of the C-C bond with respect to the main chain. It seems that the conformation is affected in quite the opposite way by the orientation conditions of the main chains during casting. Actully, either positive or negative birefringence has been observed for drawn polystyrene, depending on whether the drawing temperature is lower or higher than the glass transition temperature of polystyrene.[38,39]

C. Thermodynamic Theory of Domain Formation at a Critical Concentration

As has been pointed out in the previous sections, there is probably a critical concentration C* at which each segment of the block copolymers undergoes phase separation and aggregates into characteristic molecular micells, just as soap molecules do in aqueous solutions at a critical micelle concentration. The micelle structures thus formed may be maintained as a whole at higher concentration until the solid structures are formed.+

In this section, the manner of formation of the micelles will be discussed in terms of an equilibrium at the critical concentration in order to present a mechanism for the formation of the three types of fundamental domain structures in terms of molecular and thermodynamic parameters.

Let us introduce three types of micelle, namely, as illustrated in Fig. 10, spherical, rodlike, and alternating lamellar micelles, which correspond to the three types of fundamental domain structures that can form the domain structure at the critical concentration by hexagonal close-packing (spherical and rodlike micelles) or by piling up (lamellar micelles).

+ There has been a quite opposite proposal by Skoulios *et al.*[40] that the micelle structure must be changed stepwise from the cylinder (rod) via the sphere to the lamellar form with increasing concentration for a system of cruciform block copolymers of propylene oxide with ethylene oxide in water. In addition, there has been an early study by Bresler *et al.*,[41] suggesting different micelle structures for styrene-isoprene block copolymers, B in A modification and A in B modification, from selective solvent systems.

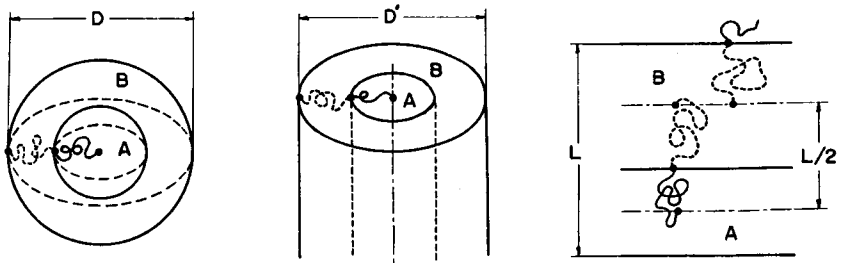

(a) spherical micelle (b) rod-like micelle (c) lamella-like micelle

Fig. 10. Schematic representations of three types of micelles and molecular orientations within the micelles (component A dispersed in component B): (a) spherical micelle; (b) roadlike micelle; (c) alternating lamellar micelle.

It may be assumed that when A-B block copolymer chains aggregate into such a micelle, phase separation occurs so as to form an interface and to arrange all junction points of the copolymer chains on the interfaces. The area of the interface per unit volume may be evaluated from dimensions, D, D', or L of the respective micelles, as indicated in Fig. 10, and the volume fraction V_A of a block segment A relative to the total volume occupied by the copolymer chain at the critical micelle concentration, unless the volume fraction is changed by the micelle formation. V_A is defined by means of the volumes of spheres whose diameters are equal to the root mean square radius of gyration of the block segments.

The Gibbs free energy G per unit volume for the formation of respective micelles may be given by:

for the spherical micelle:

$$G_s=6V_A^{2/3}(1/D)\Delta W + (3/2)kTN\left[\frac{D^2}{4}\left\{\frac{(1-V_A^{1/3})^2}{\sigma_B^2 n_B a_B^2}+\frac{V_A^{2/3}}{\sigma_A^2 n_A a_A^2}\right\}-2\right] \quad (1\,a)$$

for the rodlike micelle:

$$G_r=4V_A^{1/2}(1/D)\Delta W + (3/2)kTN\left[\frac{D'^2}{4}\left\{\frac{(1-V_A^{1/2})^2}{\sigma_B^2 n_B a_B^2}+\frac{V_A}{\sigma_A^2 n_A a_A^2}\right\}-2\right] \quad (1\,b)$$

for the lamellar micelle:

$$G_l=2(1/L)\Delta W + (3/2)kTN\left[\frac{L^2}{4}\left\{\frac{(1-V_A)^2}{\sigma_B^2 n_B a_B^2}+\frac{V_A^2}{\sigma_A^2 n_A a_A^2}\right\}-2\right] \quad (1\,c)$$

where ΔW is the interfacial contact energy between the two components per

unit area (which is the contact energy difference between unlike segments in the sense of the quasi-chemical approach and may be repulsive for incompatible components), N is the number of copolymer chains per unit volume, σ_i^2 is a parameter characterizing the effect of solvent in terms of a ratio of the mean square of the end-to-end distance of the i-block at the critical micelle concentration to that of the chain with freely jointed segments, $\langle R_i^2\rangle/\langle R_i^2\rangle_f$, n_i is the degree of polymerization of the i-block sequence having monomer length a_i, k is the Boltzmann constant, and T is the casting temperature.

For the derivation of the free energy of the micelle formation given by Eqs. (1), the reference state was taken as the virtual one with N chanins of A-homo-polymer, with $\langle R_A^2\rangle$, and N chains of B-homo-polymer, with $\langle R_B^2\rangle$, in a complete phase separation into macroscopic domains. The entropy change per copolymer chain was approximated by simply assuming that the copolymer chain is composed of two Gaussian chains of A and B homo-polymers, neglecting the effect of the junction between the A and B blocks to form the copolymer chain; *i. e.*,

$$\Delta S = \sum_{i=A,B} \Delta S_i = -(3/2)k \sum_{i=A,B} (r_{i,2}^2 - r_{i,1}^2)/(\sigma_i^2 n_i a_i^2) \tag{2}$$

where $r_{i,1}$ and $r_{i,2}$ are the end-to-end distances of the i-block at the reference state and in the micelle, respectively. The end-to-end distance, $r_{i,2}$, in the micelle formation was also simply approximated so that the junction point is fixed at the interface of respective micelles, while the ends of each block chain are fixed at particular points in the micelles, as illustrated in Fig. 10. That is, for spherical and rodlike micelles, the end of an A block is at the center of the micelle and the end of a B block is at the point on the outer surface of the respective micelle located radially through the junction point, if the micelles are formed of component A in component B. For the alternating lamellar micelles the ends of each chain are at points in the center layer of each lamella which define a line perpendicular to the interface through the junction point. The approximation of $r_{i,2}$ is very crude, giving a too high density at the center of the spherical and rodlike micelles and a too low density at the outer surface of the micelles. A different approach for evaluating the configurational entropy has been proposed by Meier[42] using a diffusion equation to represent chain perturbation so as to make the density within the spherical domain uniform in the solid state.

Fig. 11 shows the free energy curve derived from Eqs. (1) as a function of micelle size. The curve, which has a free energy trough as a result of the summation of the first term (hyperbolic decrease with micelle size) and the

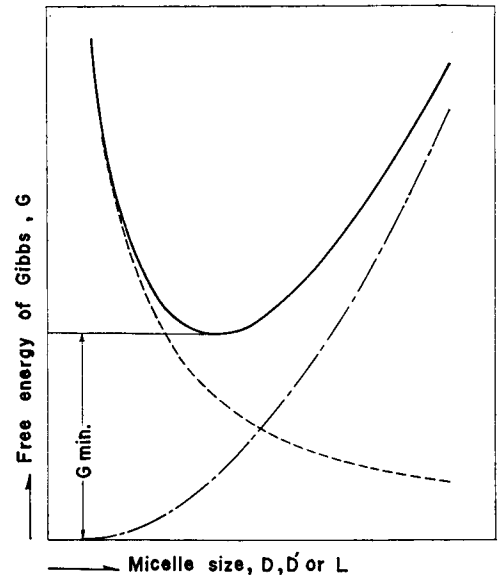

Fig. 11. Qualitative illustration of the relationship between the free energy of micelle formation G, and the size of micelle, D, D' or L.

second term (2 nd power increase with micelle size) on the right hand side of Eqs. (1), indicates that the micelle should have the size giving the minimum free energy G_{min}. In addition, it may be noted that the minimum free energy is retained as positive in contrast to a mechanical mixture of two incompatible components, for which the free energy change on mixing must be zero as a result of the complete phase separation. In other words, the microphase separation to form micelles of particular size is the most stable for an A-B block copolymer, in contrast to complete phase separation into macroscopic domains, which is the stable state for a mixture of the incompatible A- and B-homo-polymers.

More quantitative evaluation of the conditions for the minimum free energy can be made by differentiating Eqs. (1) with respect to the micelle size as follows:

$$D_{G_{min}}=f_s(\phi, \sigma, n)\Upsilon,$$

where f_s is given by

$$f_s\equiv\left[8{V_A}^{2/3}/\left\{\frac{(1-{V_A}^{1/3})^2}{{\sigma_B}^2 n_B {a_B}^2}+\frac{{V_A}^{2/3}}{{\sigma_A}^2 n_A {a_A}^2}\right\}\right]^{1/3} \tag{3 a}$$

$$D'_{G_{min}}=f_r(\phi, \sigma, n)\Upsilon,$$

where f_r is gigen by

$$f_r\equiv\left[(16/3){V_A}^{1/2}/\left\{\frac{(1-{V_A}^{1/2})^2}{{\sigma_B}^2 n_B {a_B}^2}+\frac{{V_A}^2}{{\sigma_A}^2 n_A {a_A}^2}\right\}\right]^{1/3} \tag{3 b}$$

$$L_{Gmin}=f_i(\phi, \sigma, n)\gamma,$$

where f_i is given by

$$f_i\equiv\left[(8/3)/\left\{\frac{(1-V_A)^2}{\sigma_B^2 n_B a_B^2}+\frac{V_A^2}{\sigma_A^2 n_A a_A^2}\right\}\right]^{1/3} \tag{3c}$$

where

$$\gamma^3=\Delta W/kTN$$

and

$$\sigma=\sigma_B/\sigma_A.$$

Eqs. (3) predict that the equilibrium size of the micelle increases with the cube root of the degree of polymerization ($n=n_A+n_B$) through f_i and also with the cube root of N, which must be a function of n through γ, with increasing ΔW, and with decreasing casting temperature T, provided that the temperature dependence of σ and ΔW are negligibly small. The ΔW dependence means that the more incompatible are the A and B components, the larger are the micelles.

By substituting Eqs. (3) into the respective Eqs. (1), the minimum values of the free energy for the formation of the respective types of the micelles, $G_{i,min}$ are given by

$$G_{s,min}=\{3V_A^{2/3}f_s^{-1}-(1/\gamma^2)\}3kTN\gamma^2 \tag{4a}$$

$$G_{r,min}=\{2V_A^{1/2}f_r^{-1}-(1/\gamma^2)\}3kTN\gamma^2 \tag{4b}$$

$$G_{l,min}=\{f_l^{-1}-(1/\gamma^2)\}3kTN\gamma^2 \tag{4c}$$

Comparison of $G_{i,min}$ among the three types of micelle can be made by examining the first term of the right hand side of Eqs. (4). Fig. 12 shows the above relative values of minimum free energies as a function of the weight fraction of the A-block segment, ϕ_A, where the numerical values, $\sigma_B/\sigma_A=1$, $a_A=a_B$, and $m_A/m_B=104/68$, are assumed for comparing the results with styrene-isoprene block copolymers cast from toluene solutions. Since the formation of micelles having the lowest relative value of the minimum free energy at a given weight fraction ϕ_A should predominate (as illustrated by thicker lines in the figure) at the equilibrium state at C* and T, it appears that the type of micelle, and hence the resulting domain structure in the film specimen, changes in order from spherical to rodlike to alternating lamellar with increasing ϕ_A. These expectations agree at least qualitatively with the experimental results, shown in Fig. 3. The values ϕ_1 and ϕ_2 indicated in the figure give an upper (lower) limit of the weight fraction of the block segment for the formation of each particular type of micelle.

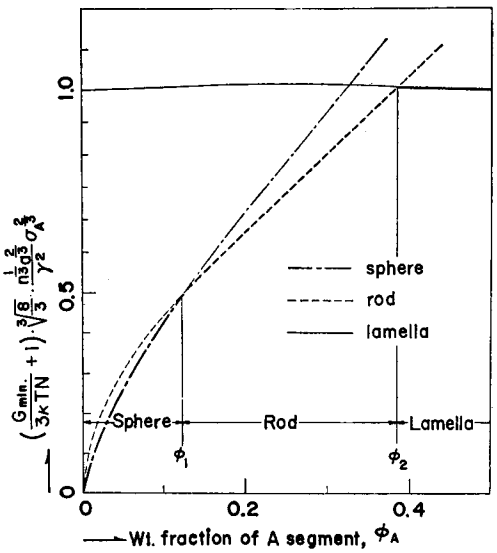

Fig. 12. Relationship between the relative minimum free energy of micelle formation (A dispersed in B) and the weight fraction ϕ_A of A blocks (with assumed values, $\sigma_B/\sigma_A=1$, $a_A=a_B=$a, and $m_A/m_B=104/68$).

The free energy minimum for micelle formation may be the most characteristic thermodynamic features of an A-B block copolymer. It is treated in this article as an entropic contribution to the free energy of micelle formation (the second term on the lefthand side of Eqs. (1)) which opposes the phase separation due to the incompatibility of the two components (the first term on the left hand side of Eqs. (1)), *i.e.*, the block segments are expected to orient to a considerable extent along the direction perpendicular to the interface between the two components. This particular orientation-aggregation of the block chains at the interface must be reflected in the rather small ratio of the dimension of the effectively occupied area per chain block at the interfaces to that of the domain structure, as illustrated in Fig. 8, and must further cause the bulk properties of the block copolymer to differ from those of mechanical mixtures of the corresponding homo-polymers, especially for the specimens with alternating lamellar structure which have much higher free energy, as shown in Fig. 12, than the others.[43]

In the above thermodynamic treatment, micelle formation was mainly discussed in terms of micelles of component A dispersed in component B. The opposite case of component B dispersed in component A can be similarly treated. The result is shown in Fig. 13 over the whole range of ϕ_A; plots are given for those values of $(\sigma_B/\sigma_A)^3$ varying from 1/2 to 2, $a_A=a_B=a$, and $m_A/$

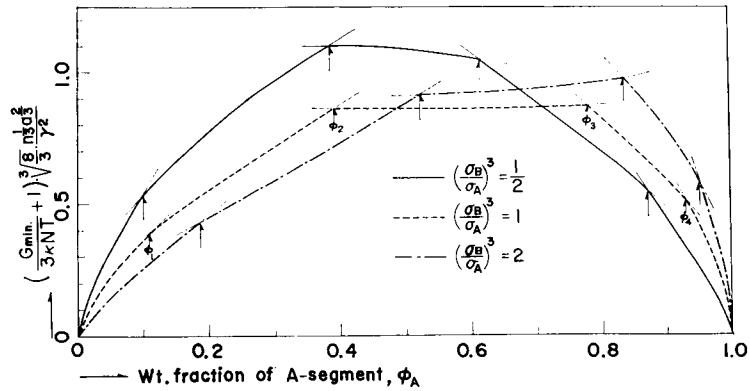

Fig. 13. Effect of sovent (relative solvation power σ_B/σ_A) upon the relationship between the relative minimum free energy of micelle formation and the weight fraction ϕ_A of A blocks. The change of mode of micelle formation from A dispersed in B (when ϕ_A is less than ϕ_2) to B dispersed in A (when ϕ_A is larger than ϕ_3) is indicated.

$m_B=104/68$. It may be seen that the type of micelle varies from spherical (A dispersed in B), to rodlike (A dispersed in B), to alternating lamellar (A and B), to rodlike (B dispersed in A), and to spherical (B dispersed in A) with increasing ϕ_A, and that the limiting fraction ϕ_i for each type of micelle shifts toward lower values with decreasing relative solvation power, σ_B/σ_A.

This dependence of the type of micelle on ϕ_A agrees, at least qualitatively, with the changes in the domain structures shown in Fig. 3, except for the rodlike structure of the styrene component dispersed in an isoprene matrix which was unfortunately unrealized because of the lack of the copolymer containing an adequate weight fraction. The existence of the rodlike structure, as well as the above change of domain structure as a function of ϕ_A, have been also demonstrated by Matsuo *et al.*[26] They formed the same morphological effects in *A-B*, *A-B-A*, and *B-A-B* block copolymers of styrene and butadiene, which will be discussed in the following chapter, IV, together with our results on the *A-B-A* block copolymer of styrene-isoprene-styrene.

The change of domain structure of the 40/60 block copolymer (SI-2) from the alternating lamellar structure (Fig. 3 b) to the styrene rods in an isoprene matrix (Fig. 5 c) is represented in Fig. 13 by changing the relative solvation power $(\sigma_B/\sigma_A)^3$ from unity to 2 at $\phi_A=0.4$; *i. e.*, the change of solvent from toluene (a rather good solvent for both block segments) to cyclohexane (a good solvent for the isoprene segment but a rather poor solvent for the styrene segment) may be represented in terms of the change in the relative solvation power from almost unity to larger than unity. In contrast, the change of domain structure of the 50/50 block copolymer (SI-3) from the alternating

lamellar structure (Fig. 6 a) to the isoprene spheres in a styrene matrix (Fig. 6 d) is also represented in Fig. 13 by changing the relative solvent power $(\sigma_B/\sigma_A)^3$ from unity to far less than 1/2 at $\phi_A=0.5$; *i. e.*, the change of the solvent from toluene to its mixture with MEK by a ratio of 1/8 (a good solvent for the styrene segments but a poor solvent for the isoprene segments) may be represented by shifting the plots in Fig. 13 to the left side to a considerable extent so that the limiting fraction ϕ_4 is, at least, less than 0.5.

The independence of the limiting fraction ϕ_i with respect to temperature (insensitivity of the type of micelle to casting temperature) and the dependence of the size of micelle (Fig. 10) are expected, unless ΔW and σ_B/σ_A are temperature-sensitive. This has been checked by casting the 40/60 block copolymer from toluene solution at various temperatures from 10 to 50°C. Identical structures were observed, confirming that no change of micelle type occured. However, no systematic change in the size of micelle with the casting temperature, as expected from Eqs. (3), could be observed. The dependences of the size of micelle and, subsequently, the size of domain upon the degrees of polymerization of the block segments have been discussed experimentally be Bradford and Vanzo[44] as well as theoretically by the present authors, as will be reviewed in the following chapter, IV.

It may be concluded in this chapter that one can account for the five types of fundamental domain structures and their size, obtained by casting an *A-B* type block copolymer from solutions, in terms of thermodynamic and molecular parameters, such as the incompatibility parameter ΔW between the block segments, the relative solvation power σ_i of the solvent for each block, the total chain length n of the copolymer, and the fractional composition ϕ_A of the *A* segment in the copolymer.

III. Domain Structures of a Ternary Polymer System of an A-B Type Block Copolymer of Styrene and Isoprene, Polystyrene, and Polyisoprene, Cast from Solutions.[24]

A. Experimental Procedures and Results

Most of the *A-B* block copolymers used in the previous chapter were further used in this chapter for examining the domain structures of binary or ternary polymer systems of an *A-B* block copolymer, an *A*-homo-polymer, and a *B*-homo-polymer, while an *A-B* block copolymer of 80/20 styrene-isoprene (SI-6), and homo-polystyrenes and homo-polyisoprenes differing in degree of polymerization, respectively, were newly synthesized by the anionic polymerization technique initiated by *n*-BuLi in THF at −78°C. Characterization of these

Table 2. Characterization of A-B Type Block Copolymer of Styrene-Isoprene and Corresponding Homopolymers Used.

Specimen code	$\bar{M}_n \times 10^{-4}$*	Wt fraction of styrene, %	Optical appearance of film cast from toluene
SI-6*** (80/20 Sty-Isop)	103	78**	Slightly cloudy and slightly iridescent.
PS-LL	143	100	Transparent
PS-L	60.1	100	Transparent
PS-M	18.0	100	Transparent
PS-S	3.34	100	Transparent
PI-M	39.8	0.00	Transparent
PI-LL	112	0.00	Transparent

* Measured by a high speed membrane osmometer in toluene solution at 37°C.
** Determined from UV absorption at 262 mμ in CCl_4 solution.
*** Contaminated with homo-polyisoprene having somewhat broad distribution of molecular weight.

newly synthesized polymers was performed, as in the previous chapter, by ultracentrifugation, osmotic pressure, and ultraviolet and infrared spectra, and listed in Table 2, together with their specimen codes.

The domain structures of solvent cast films of several compositions of two or three components of an *A-B* block copolymer of styrene and isoprene, homo-polystyrene, and homo-polyisoprene from their 5 % toluene solutions at room temperature were investigated under ordinary light and electron microscopes by using the OsO_4 fixation technique.

Figs. 14 through 17 show the electron micrographs of the ternary or binary system, together with the triangular diagrams indicating the composition of the systems and the optical appearance of the film specimens.

All specimens in Fig. 14 are mixtures in which the ratio of styrene to isoprene components is maintained at 73/27, which is identical with the styrene/isoprene ratio in the 70/30 block copolymer (SI-5). The molecular weights of the homo-polymers are also selected as being almost similar to those of the corresponding copolymer blocks. The method for forming the domain structure of the 70/30 block copolymer from toluene solution *i. e.*, to form spheres of isoprene component dispersed in a matrix of styrene component (Fig. 3 f and Fig. 14 a), is still maintained for the ternary mixtures along the isopleth, as seen in Figs. 14 b through 14 f. The size distribution of the domain structure is considerably broadened as the fraction of the copolymer decreases. It appears that each homo-polymer added is solubilized into respective block domains composed of like components.

For the ternary mixtures along the isopleth corresponding to the composi-

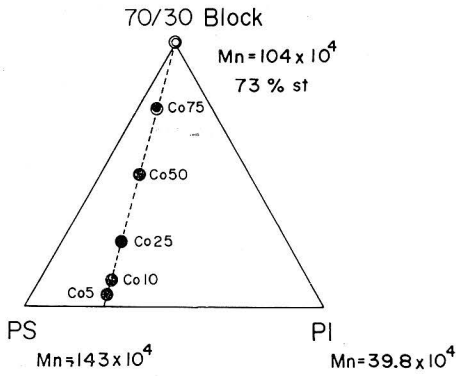

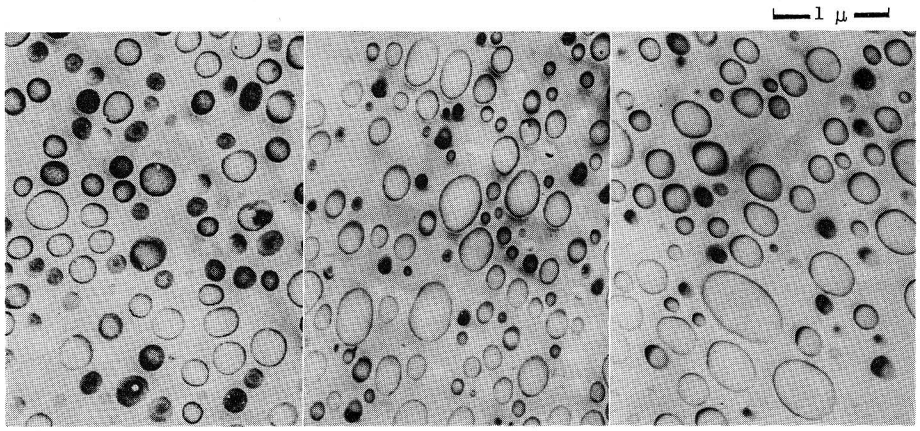

(a) (SI-4, 70/30 Sty-Isop) (b) (Co 75) (c) (Co 50)

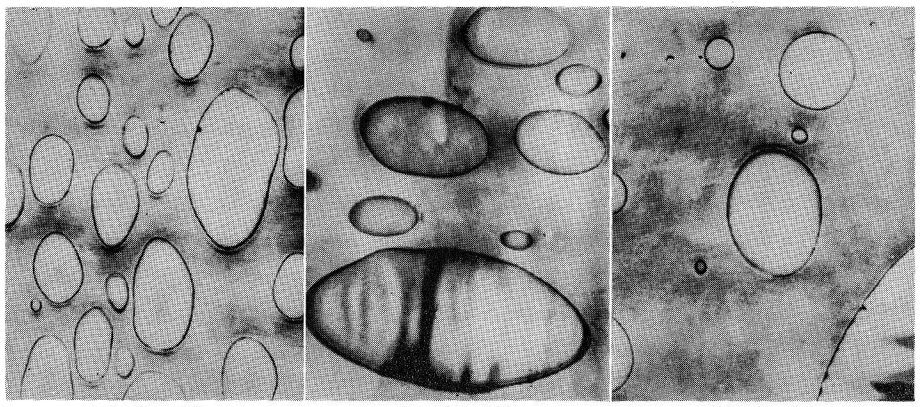

(d) (Co 25) (e) (Co 10) (f) (Co 5)

Fig. 14. Triangular diagram representing the composition in weight fractions of ternary mixtures and electron micrographs of ultrathin sections of film cast from 5 % toluene solutions and stained by OsO_4.

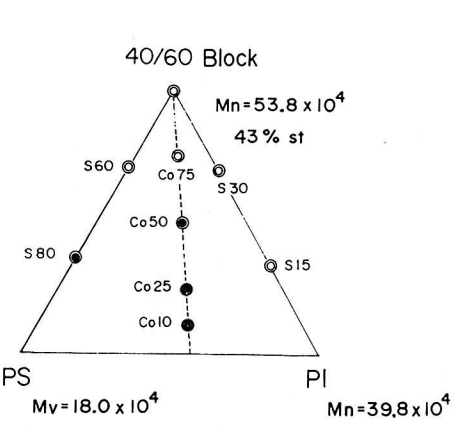

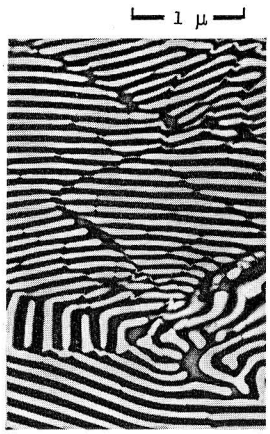

(a) SI-2, 40/60 Sty-Isop)

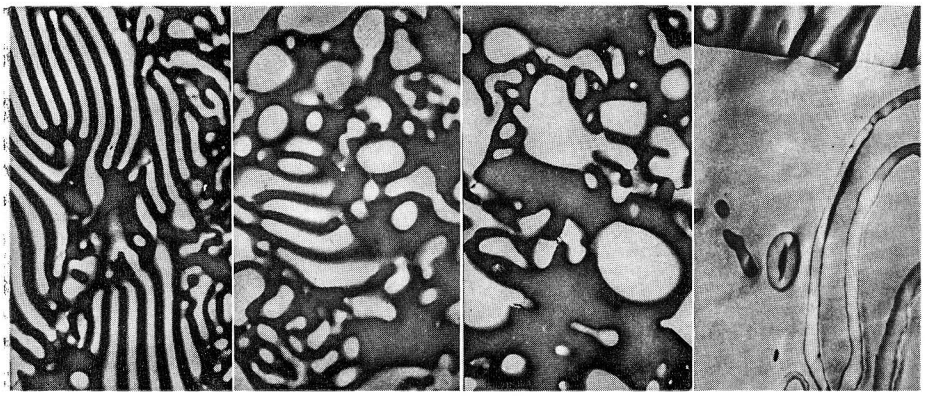

(b) (Co 75) (c) (Co 50) (d) (Co 25) (e) (Co 10)

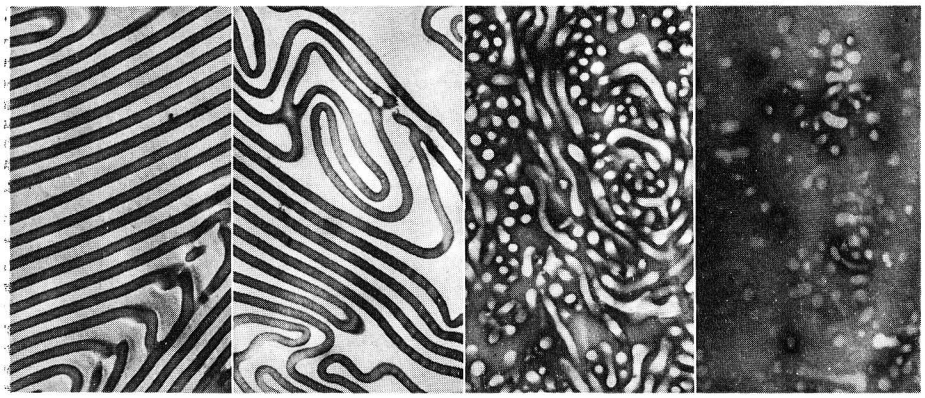

(f) (S 60) (g) (S 80) (h) (S 30) (i) (S 15)

Fig. 15. Triangular diagram representing the composition in weight fractions of ternary or binary mixtures and electron micrographs of urtrathin sections of films cast from 5 % toluene solutions and stained by OsO_4.

tion of the 40/60 block copolymer (SI-2), the original domain structure with the alternating lamellar arrangement, as seen in Fig. 3 b and Fig. 15 a, is maintained only is a large fraction of the copolymer and is gradually changed, as illustrated in Figs. 15 b through 15 e with decreasing fractions of the copolymer, to a structure of very irregular fragments of styrene component dispersed in a matrix of isoprene component. For the binary mixture of the 40/60 block copolymer with homo-polystyrene or homo-polyisoprene, where the total composition of styrene or isoprene sequences is no longer kept constant, the domain structure changes systematically with increasing fractions of styrene or isoprene sequences; *i. e.*, for the former case, the structure changes from the alternating lamellar arrangement, Fig. 15 a, to more separated lamellar arrangements, Figs. 15 f and 15 g, due to the thickening of the styrene lamella, while for the latter case, the structure changes from the alternate lamellar arrangement to styrene rods, Fig. 15 h, to styrene spheres, Fig. 15 i, both dispersed in a matrix of isoprene component. For every specimen in Fig. 15, where the molecular weights of the homo-polymers are again selected as being similar to those of the corresponding blocks of the copolymer, the solubilization of the homo-polymers into the respective block domains takes place. But the domain structure of alternating lamellar arrangement for the 40/60 block copolymer is not maintained if the copolymer fraction along the isopleth drops below around 50 %.

For the binary mixtures of the hsM-series in Fig. 16, where the 20/80 block copolymer (SI-1) is mixed with a homo-polystyrene of relatively higher molecular weight (PS-M) than that of the corresponding block of the copolymer, it is noticeable that a phase separation into the homo-polystyrene phase and the block copolymer phase occurs without any disturbance of the original domain structure of the block copolymer. This is obvious in a comparison of Fig. 16 b′, an electron micrograph of the block copolymer phase (matrix phase in Fig. 16 b), with Fig. 16 a, the original domain structure of the 20/80 block copolymer. Large ellipsoids of the homo-polystyrene component are dispersed in a matrix of the block copolymer component which forms an inherent domain structure of spheres of styrene blocks in a matrix of isoprene blocks. The same phenomena are observed in a binary mixture of the block copolymer with a homo-polystyrene of much higher molecular weight (PS-L) than the hsM-series, as illustrated in Fig. 16 f. In this case, the interface between the homo-polystyrene phase and the block copolymer phase is demonstrated clearly in Fig. 16 f′. On the other hand, when the block copolymer is mixed with a homo-polystyrene of relatively low molecular weight (PS-S) than that of the

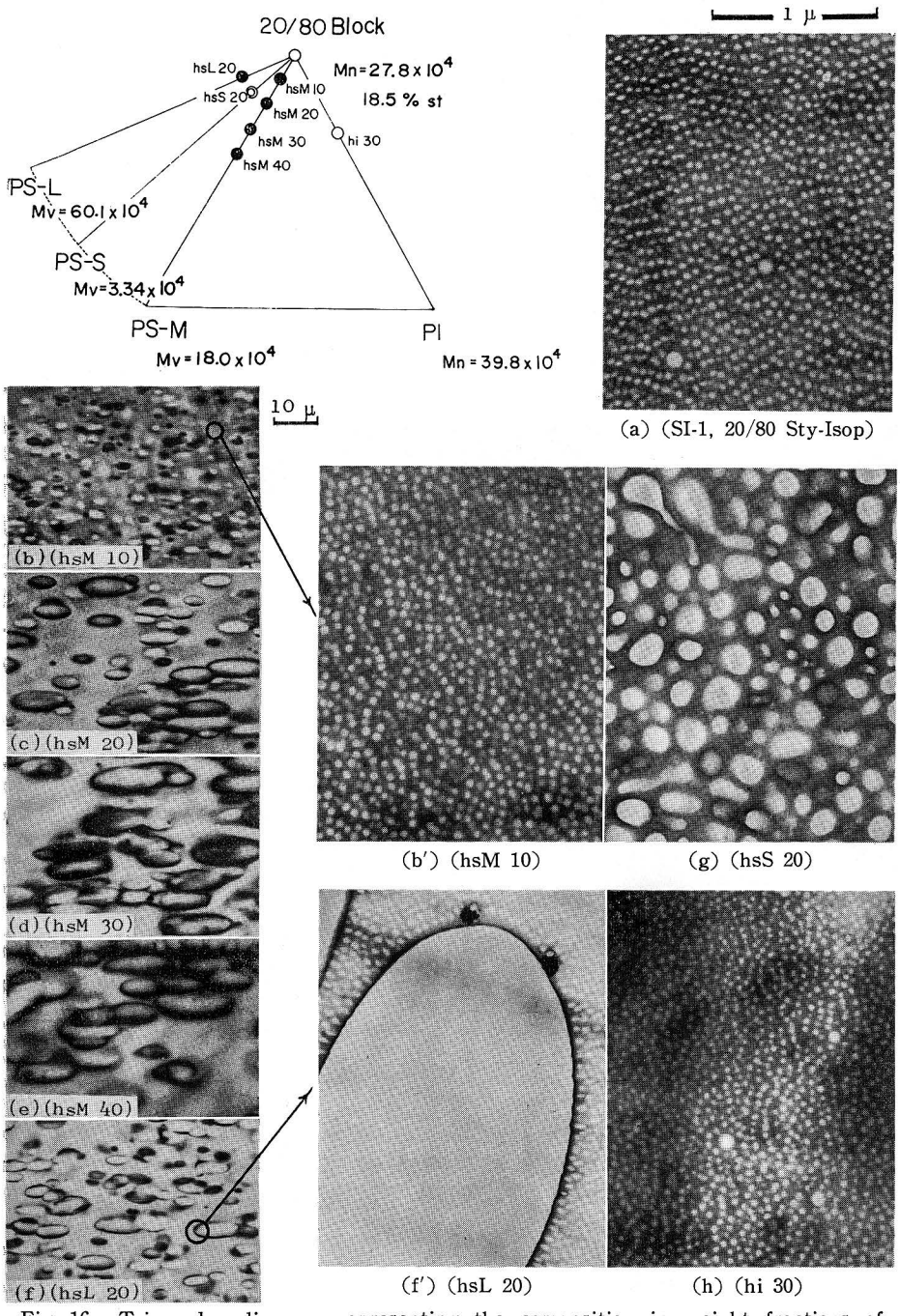

Fig. 16. Triangular diagram representing the composition in weight fractions of binary mixtures and electron and ordinary micrographs of ultrathin and thin sections of films cast from 5 % toluene solutions and stained by OsO_4.

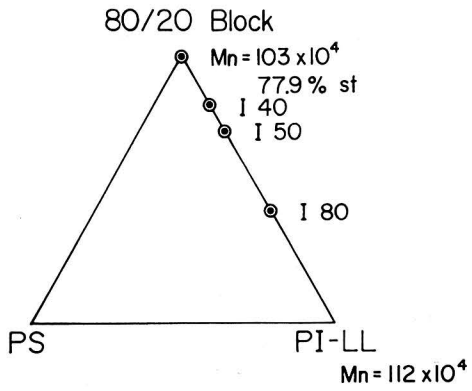

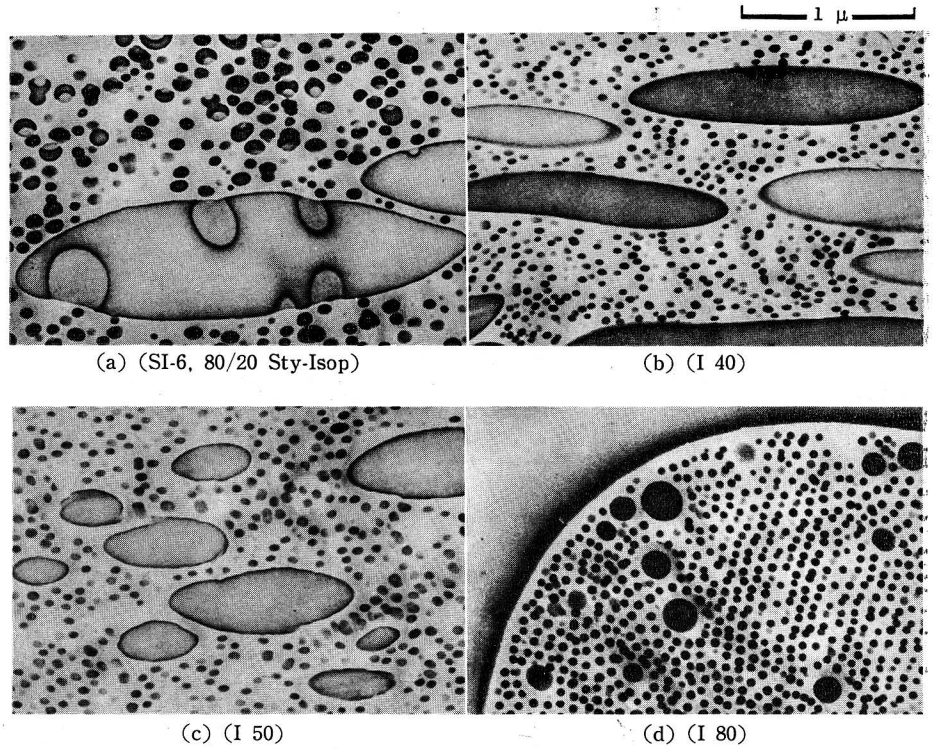

(a) (SI-6, 80/20 Sty-Isop) (b) (I 40)

(c) (I 50) (d) (I 80)

Fig. 17. Triangular diagram representing the composition in weight franctions of binary mixtures and electron micrographs of ultrathin sections of films cast from 5 % toluene solutions and stained by OsO_4.

corresponding block of the copolymer, the homo-polystyrene is solubilized into the domain of the styrene block of the copolymer, as seen in Fig. 16 g, to enlarge its spherical domain. This is in contrast to the above cases involving high molecular weight polystyrenes but is similar to the cases discussed in

connection with Figs. 14 and 15. For the binary mixtures of the 20/80 block copolymer with a homo-polyisoprene (PI-M), whose molecular weight is of the same order as that of the corresponding block of the copolymer, the homo-polyisoprene is solubilized into the matrix domain of the isoprene block of the copolymer. This increases the separation of the spheres of styrene blocks in a very quantitative manner, as seen in Fig. 16 h, in comparison with that in Fig. 16 a.

For the binary mixtures of the hiL-series in Fig. 17, where the 80/20 block copolymer (SI-6) is mixed with a homo-polyisoprene of much higher molecular weight (PI-LL) than that of the corresponding block of the copolymer, a phase separation into the homo-polyisoprene phase and the block copolymer phase occurs, in principle, similarly as in the cases of the mixtures of the 20/80 block copolymer with homo-polystyrenes of relatively higher molecular weights. Judging from a sedimentation pattern of the 80/20 block copolymer in ultracentrifugation, the copolymer is not a genuine but a contaminated block copolymer with homo-polyisoprene having a somewhat broad distribution of molecular weight around a critical value of being solubilized into the domain of the corresponding block of the genuine block copolymer. As can be seen in Fig. 17 a, an original domain structure of the 80/20 block copolymer, there appear, at least, two types of isoprene domains, *i.e.*, very large ellipsoidal domains and rather small but not unisized spherical domains. The large ellipsoidal domains must have arisen from the segregation of homo-polyisoprene of relatively higher molecular weight from the copolymer, while the small spherical domains must have arisen from the solubilization of homo-polyisoprene of relatively lower molecular weight into domains of corresponding block segments of the genuine copolymer. On the other hand, it is apparent, as seen in Figs. 17 b through 17 d, that the large ellipsoidal domain becomes dominant (Fig. 17 b) and eventually occupies a matrix phase of the mixed system (Fig. 17 d), and that the small spherical domain becomes smaller but more uniform in size, both occurring when the 80/20 block copolymer was mixed with another homo-polyisoprene of much higher molecular weight (PI-LL). This suggests that the small but uniform spherical domains in Figs. 17 b through 17 d must be composed of the corresponding block segments of the genuine block copolymer and that the homo-polyisoprene contaminating the genuine block copolymer is solubilized into the large ellipsoidal domain of homo-polyisoprenes.

The above results indicate that when the molecular weight of the homo-polymer added is of the same order or less than that of the corresponding block of the copolymer, the solubilization of the homo-polymer into the domain

of the corresponding block takes place. In this case, the two incompatible homo-polymers can be blended well with each other by adding the corresponding block copolymer. That is, the block copolymer behaves just like an emulsifier restraining the phase separation of the homo-polymers into their macroscopic domains. But when the molecular weight of the homo-polymer added is much higher than that of the corresponding block, the copolymer can no longer act as the emulsifier. Namely, the block copolymer behaves as if it were incompatible with the corresponding homo-polymers and loses the tendency to incorporate the sequences of like homo-polymers.

The inherent manner of domain formation of the block copolymer from its solution was discussed in the previous chapter in terms of the thermodynamic and molecular parameters. Results presented here suggest that when the above condition for the solubilization of homo-polymers into the block domains of the copolymer is satisfied and the fraction of the copolymer is kept relatively large, the same manner of domain formation may be maintained even for the ternary and binary systems. Namely, the formation of five types of fundamental domain structures, *A* spheres in *B* matrix, *A* rods in *B* matrix, alternating lamellar arrangement, *B* rods in *A* matrix, and *B* spheres in *A* matrix, may be achieved, depending upon the total ratio of *A* sequences to *B* sequences in the system.

This is demonstrated schematically in Fig. 18, using a triangluar phase diagram, in which the chain line indicates the isopleth, keeping the total sequence ratio identical with that of the *A-B* block copolymer. Thus, for the diagram from Figs. 18 a through 18 c the composition of the *A-B* block copolymer

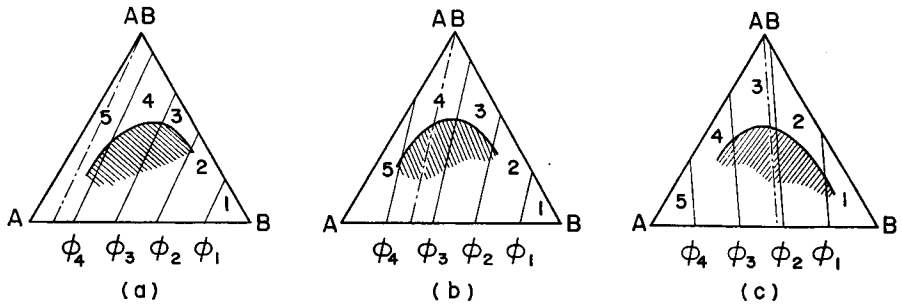

Fig. 18. Triangular phase diagram representing the mode of domain structures formed from solutions of the three polymers in a common solvent, where the chain line indicates an isopleth, and the area 1 corresponds to the domain structure of A spheres dispersed in B matrix, the area 2 to A roods in B matrix, the area 3 to the alternating lamellar arrangement, the area 4 to B rods in A matrix, and the area 5 to B spheres in A matrix.

changes from *A* rich copolymer to rather *B* rich copolymer. In each diagram the area 1 corresponds to the domain structure of *A* spheres dispersed in *B* matrix, the area 2 to *A* rods in *B* matrix, the area 3 to alternating lamellar arrangement, the area 4 to *B* rods in *A* matrix, and the area 5 to *B* spheres in *A* matrix. The above domain formation may be achieved stably only outside of the hatched area. The results for the ternary system in Fig. 14 correspond to the area 5 in Fig. 18 a, when the component *A* is styrene. The results for the binary system in Fig. 15 along the sides of 40/60 Block-PS and 40/60 Block-PI correspond to the side *AB-A* within the area 3 and the side *AB-B* in Fig. 18 c, respectively, when the component *A* is styrene.

The optical appearance of the cast films is indicated in terms of the circular symbols in the triangular diagrams; an open circle designates transparent, a double open circle designates transparent but iridescent, a dot-open circle designates cloudy and iridescent, and a dot designates opaque. Judging from the relationship between the optical appearance of cast films represented by the circular symbols and their domain structures, it may be said that the transparency depends on the size and distribution of the domain structure and that the iridescent phenomena are due to the periodic nature of the structure, both in relation to the wave length of visible rays.

B. Domain Fofmation Mechanism of Ternary or Binary System

1. POO-emulsion and Emulsifying Efficiency of Block Copolymer

Molau *et al.*[7-9] demonstrated a mechamism for the domain formation of rubber particles during the polymerization of solutions of rubber in vinyl monomers. They showed that a polymeric oil-in-oil emulsion, produced after a phase inversion at the beginning of the polymerization, is transformed into a solid structure as the polymerization proceeds. Assuming that the residual monomer at the stage of POO-emulsion is considered as a casting solvent, and that the graft copolymer of the rubber and vinyl polymer produced during the polymerization is an *A-B* block copolymer, the polymerization process may be treated as similar to the solvent casting process in our experiments. Consider the process of casting from a dilute solution, the three polymer solutes, *A-B* block copolymer, *A*-homo-polymer, and *B*-homo-polymer, in a common solvent to form the ternary solid. Here the POO-emulsion thus formed is maintained as a whole at a higher concentration until the solid structure is achieved. The block copolymer chains are squeezed out on the interface of the POO-emulsion (see Fig. 19) as a result of the complete immiscibility[45,46] of the unlike sequences at sufficiently high polymer concentration.

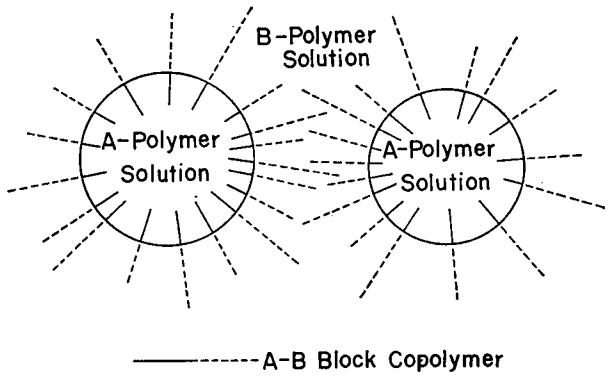

Fig. 19. Polymeric oil-in-oil emulsion of A droplets in B solution type, stabilized by the A-B type block copolymers accumulated at the interface beetween the spherical droplets and the matrix.

The formation of a micro-heterogeneous domain structure of two incompatible components by the solvent casting of the three polymer solutes, as demonstrated in Figs. 14 through 17, suggests the emulsifying effect of the *A-B* block copolymer. This effect must now be discussed in terms of the POO-emulsion state. The uniformity of the domain size as well as the regularity of the domain shape in the cast films suggest that a high degree of stability of the POO-emulsion is achieved by the coalescence barrier which prevents demixing of the system. This is indicated by the data in the figures, especially when the fraction of the block copolymer in the system is relatively large. In addition to Molau's discussion concerning the sources of the coalescence barrier in POO-emulsion,[7-9] the concept of the entropic repulsion between approaching droplets, which are covered by block chains of opposite component, would have to be taken into account in the way proposed by Clayfield[47] and Meier.[48] These workers consider the repulsive force between particles, which absorb polymer chains on each surface, in terms of the decrease in configurational entropy of the chains due to the loss of possible configurations as the space available to the chains is reduced between approaching particles.

A broad size distribution with decreasing fractions of the *A-B* block copolymer added is observed along the isopleth in Fig. 14. Such behavior can be explained in terms of a random aggregation of the droplets of the POO-emulsions having low coalescence barriers due to the lack of copolymer chains being supplied on the unit surface area of the droplets. The irregularity of domain shape, which is observed along the isopleth in Fig. 15, may also be explained in terms of the lack of sufficient copolymer chains because of the

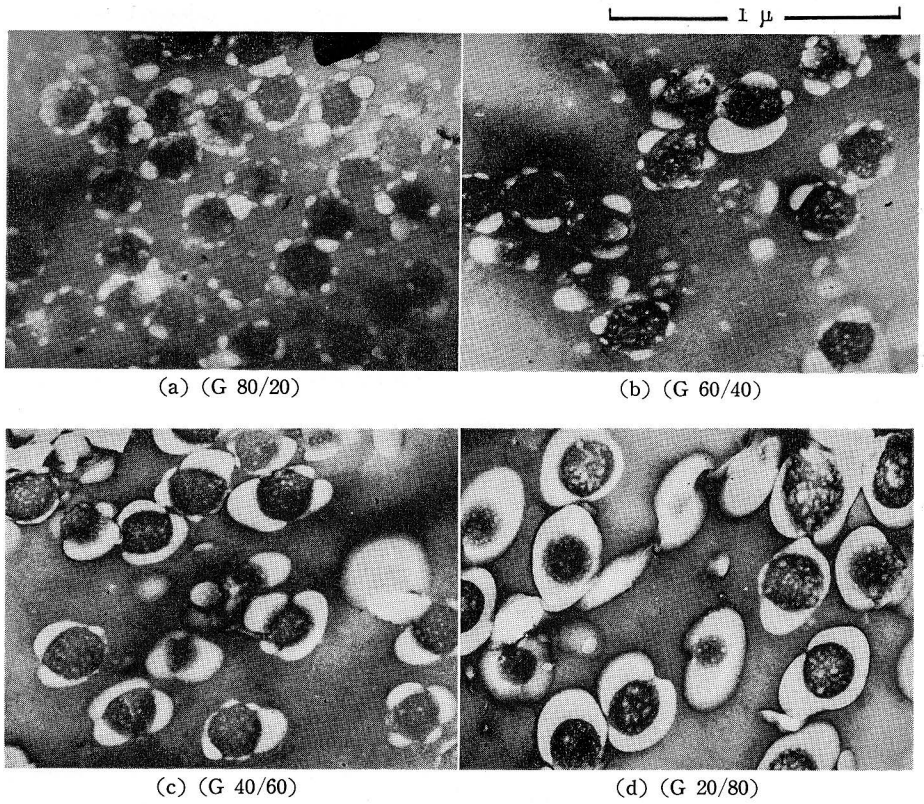

Fig. 20. Electron micrographs of ultrathin sections of a series of ABS lattices embedded in a mixture of polybutadiene and agar-agar and stained by OsO_4. The series of ABS lattices was made so that the degree of grafting of styrene-acrylonitrile copolymer onto the surface of polybutadiene lattices varies from 20 to 80 wt% in order from (G 80/20) to (G 20/80).

relatively large interfacial area of the alternating lamellar arrangement compared to the spherical domain structure.

Fig. 20 shows electron micrographs of ultrathin sections of a series of ABS lattices embedded in a matrix of polybutadiene and agar-agar and stained by OsO_4. The series of ABS lattices was made by a particular grafting technique in an emulsion system of polybutadiene lattices dispersed in a medium containing styrene and acrylonitrile monomers so that the grafting occurs mostly onto the surface of the lattices, not within the lattices, and that the degree of grafting varies from 20 to 80 wt% for the series. As seen in the figure, polybutadiene spheres (black spheres stained by OsO_4) are surrounded by a thicker layer of the grafted chains of styrene-acrylonitrile copolymer (white layer unstained by OsO_4) as the degree of grafting increases.[18] Fig. 21 also shows

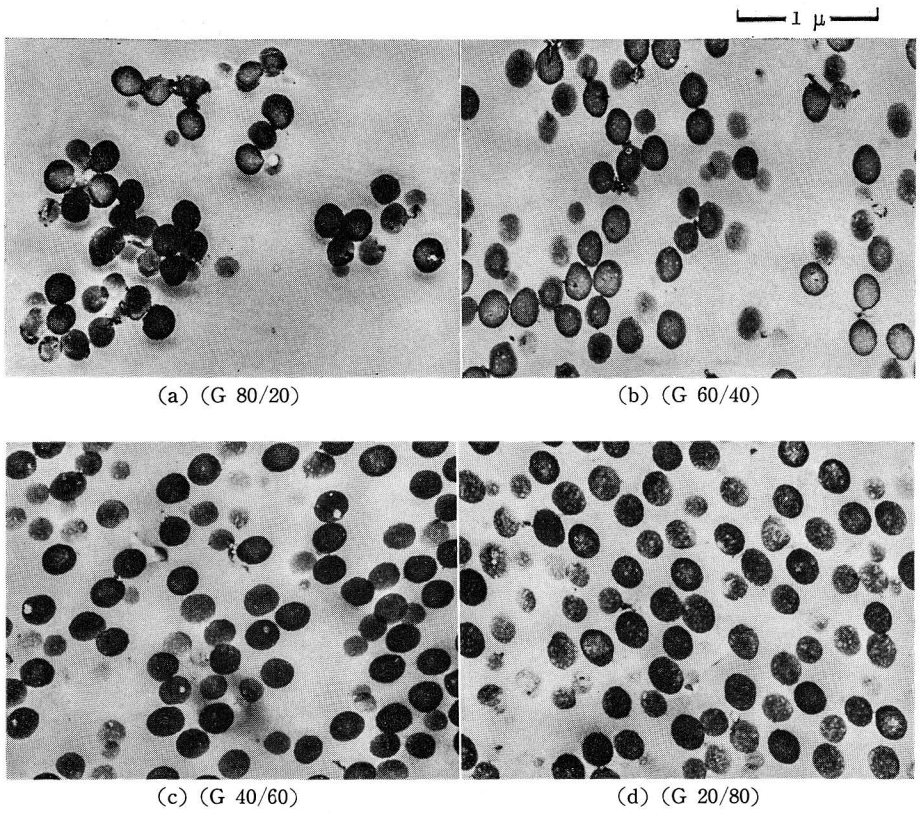

Fig. 21. Electron micrographs of ultrathin sections of about 350 Å thick cut normal to the surfaces of a series of film specimens cast from 5 % monochlorobenzene solutions of mixtures of a styrene-acrylonitrile copolymer with each ABS latex in Fig. 20 and stained by OsO_4. For mixing the two components, the fraction of each latex was controlled so that the weight fraction of polybutadiene was always kept constant, as a whole, as 20 wt % for every specimen.

electron micrographs of ultrathin sections of a series of film specimens cast from 5 % monochlorobenzene solutions of mixtures of a styrene-acrylonitrile copolymer, whose molecular composition is the same as that of the grafted copolymer, with each ABS latex. For mixing the two components, the fraction of each ABS latex was controlled so that the weight fraction of polybutadiene is always kept constant, as a whole, at 20 % for each specimen. As seen in the figure, the spherical domains of polybutadiene (black spheres stained by OsO_4) which are dispersed in a matrix of styrene-acrylonitrile copolymer (while the matrix remains unstained by OsO_4), are very uniform in size for every specimen, but less uniformly dispersed as the degree of grafting of the ABS latex decreases. This systematic change of dispersity should be understood,

as discussed previously, in terms of the coalescence barrier which prevents demixing of the POO-emulsion of ABS lattices in the monochlorobenzene solution of the styrene-acrylonitrile copolymer during the casting of the system. That is, the greater the degree of grafting on the ABS lattices, the stronger the entropic repulsion between approaching droplets of the ABS lattices becomes, resulting in the more uniform dispersion of the spherical domains of polybutadiene in the matrix of styrene-acrylonitrile copolymer.

2. *Relationship between C* and the Binodal Surface of the Four Component System; A-B Type Block Copolymer, A Polymer, B Polymer, and Solvent.*

The next problem to be discussed here is the criterion for the solubilization of the four component system: *A-B* block copolymer, *A*-homo-polymer, *B*-homo-polymer, and solvent. For the four component system, there may also be a critical concentration of total polymer, C*, at which the POO-emulsion is formed as a result of microphase separation. When C* of the four component system is at C_1* in Fig. 22, the solubilization has to occur in the following fashion. If C* is outside of the binodal surface of the four component phase diagram, the solution is homogeneous at C* and the three polymer solutes cooperate together for the micelle formation which results in the POO-emulsion stabilized by the copolymer. On the other hand, if the C* is at C_2* in the diagram of Fig. 22, *i.e.*, inside of the binodal surface, the phase separation into the copolymer solution and the homo-polymer solutions occurs before C* is reached during the casting process. Consequently, the block copolymer forms an inherent domain structure undisturbed by the homo-polymers, re-

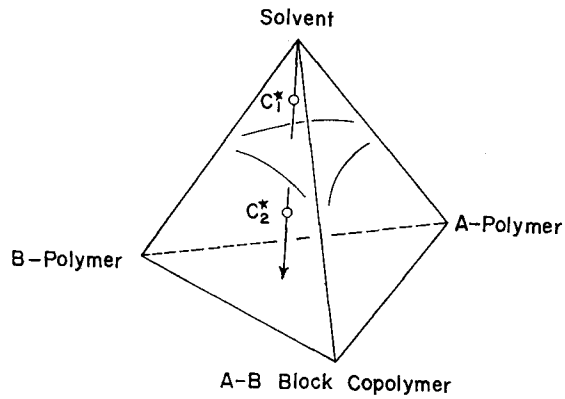

Fig. 22. Schematic representation of the binodal surface in the phase diagram of a four component system, where *C** is the critical micelle concentration of the system.

sulting in a separation into a macroscopic phase of the copolymer and the homo-polymers. Therefore, the problem is one of relating C* to the binodal surface of the system.

A theoretical derivation of C* may be performed by developing Meier's formulation,[42] but this seems unlikely to give an analytical solution. Experimental values of C*, such as those obtained by Vanzo as around 9 % for a system of ethylbenzene and a block copolymer of styrene and butadiene,[6] may be utilized.

3. Phase Equilibria in the Ternary System; A-B Type Block Copolymer, B-Polymer, and Solvent.

Derivation of the binodal surface of the four component system may be very complicated. Even for the ternary system, it may still be difficult to get an analytical representation of the binodal curve. However, in considering the three components without one of the homo-polymers, the generality for the problem is not lost, and a plait point of the system composed of *A-B* block copolymer, *B*-homo-polymer, and solvent may be approximated by using the Flory-Huggins theory[49] and the dilution approximation[46] as follows:[24]

$$C_c = 1 - (v_s)_{crit.} = (1+1/\sqrt{r})^2/(2\chi\phi_A) \tag{5}$$

where C_c is the total polymer concentration at a plait point, and $(v_s)_{crit.}$ is the volume fraction of the solvent in the ternary system at the critical concentration. Eq. (5) may predict the compatibility of the *A-B* type block copolymer with the *B*-homo-polymer in a solution of common solvent as a function of the ratio of the degrees of polymerization, r, the volume fraction of *A*-segment within the copolymer, ϕ_A, and the copolymer-homo-polymer interaction parameter, χ.

Consequently, one may judge roughly whether the solubilization occurs or not, from the following condition:

$$2\chi\phi_A C^* \gtrless (1+1/\sqrt{r})^2 \tag{6}$$

IV. Domain Formation Mechanism of an A-B-A Block Copolymer of Styrene-Isoprene-Styrene Cast from Its Solutions.[25]

In this chapter, the mechanism of domain formation when an *A-B-A* block copolymer of styrene-isoprene-styrene separates from solution will be investigated in comparison to that of the *A-B* block copolymer of the same components, and differences in some bulk properties, such as swelling properties, will be discussed in relation to the difference of molecular arrange-

ments for forming the domain structures between the two types of the block copolymers.

A. Experimental Procedures and Results

1. Preparation of an A-B-A Type Block Copolymer of Styrene-Isoprene-Styrene

A-B-A block copolymers of styrene-isoprene-styrene were synthesized by a "living polymerization" technique using the copolymerization apparatus described in Fig. 1 in the previous chapter. However, a bifunctional initiator, tetramethylene di-Li, was used instead of the monofunctional initiator *n*-BuLi used previously for synthesizing *A-B* block copolymers. The fraction of *A* and *B* block segments was varied from zero to unity.

Polymerization of isoprene monomer, and then, styrene monomer, was performed in the block copolymerization apparatus. That is, the polymerization of the isoprene monomer was, first, carried out by mixing the initiator solution (tetramethylene di-Li solution in heptane) and the isoprene monomer in THF at a low temperature, around —45°C. The reaction, which gave a pale yellow color, was, allowed to continue for about 50 hrs at the same temperature until the monomer was completely consumed. Then, block copolymerization of styrene to the polyisoprene block sequence was carried out at the temperature of dry ice-methanol (*ca.* −60°C) by adding styrene monomer to the solution containing (living) polyisoprenyllithium anions as the initiator. The reaction, which gave a reddish yellow color, was terminated by adding *n*-butanol solution in THF after about 30 min.

The copolymers thus obtained were characterized by ultracentrifugation, osmotic pressure, and infrared and ultraviolet spectroscopy, similarly as in the previous chapter for *A-B* block copolymers, for determining non-contamination with homo-polystyrene and *A-B* block copolymer, number-average mole-

Table 3. Characterization of A-B-A Type Block Copolymers of Styrene-Isoprene-Styrene Used.

Specimen code	$\bar{M}_n \times 10^{-4}$*	Wt fraction of styrene, %**	Optical appearance of film cast from toluene
SIS-1 (5/90/5 S-I-S)	29.7	9.5	Transparent
SIS-2 (10/80/10 S-I-S)	59.5	23.0	Transparent but slightly iridescent.
SIS-3 (25/50/25 S-I-S)	46.8	47.0	Transparent but iridescent.
SIS-4 (35/30/35 S-I-S)	70.2	72.0	Slightly cloudy.

* Measured by a high speed membrane osmometer in toluene at 37°C.

** Determined from UV absorption at 262 mμ in CCl_4 solution.

cular weight, fractional composition of the styrene component, and molecular structure of the isoprene segment, respectively. The results obtained are listed in Table 3, together with the specimen codes.

The copolymers thus prepared were cast into films of about 0.2 mm thick by pouring relatively dilute solutions of about 5 % concentration in various solvents onto a glass plate floating on mercury and evaporating the solvents gradually at about 30°C. The film specimens thus formed were further dried under a vacuum of about 10^{-4} mmHg at the casting temperature for a few days.

2. Electron Microscopy

The domain structure of the film specimens thus prepared was investigated with an electron microscopy using the OsO_4 fixation technique. Ultrathin sections of about 350 Å thickness were cut by an LKB ultramicrotome.

Change of Domain Structure with Fraction of Block Sequences. For specimens cast from a 5 % toluene solution, the domain structure resulting from microphase separation of the block segments was observed. As shown in Fig. 23, the domain structure changed in a systematic manner with increasing fractions of styrene compnent. The junctions between the polystyrene and polyisoprene segments in each chain should be distributed along the boundary between the two phases.

The domain structure of film specimen SIS-1 (Fig. 23 a) may be characterized as spheres of styrene component dispersed in a matrix of isoprene component. The domain structure of SIS-2 (Fig. 23 b) reveals only two kinds of patterns of the unstained styrene component; *i. e.*, circular patterns almost identical in diameter and slightly curved stripes of various length and almost the same width as the diameters of the circles. These results suggest that the electron micrograph should be understood as a sectional view of almost identical and slighly curved rods of styrene component arranged nearly parallel in a matrix of isoprene component.

On the other hand, the structure of SIS-3 (Fig. 23 c) is characterized by alternating stripe patterns of each component. It was clarified stereographically that the alternating stripe pattern is a sectional view of an alternating lamellar arrangement of the two components; *i. e.*, each component separating into lamellae oriented roughly parallel to the film surface. The iridescent color effect, which was pointed out in the previous chapter for domain formation in *A-B* type block copolymers, was also observed here, especially for the block copolymer SIS-3 having a very periodic nature in its structure, in the solid as well as in the swollen polymer when the concentration was greater than a critical concentration of about 10 %. The domain structure of SIS-4 (Fig.

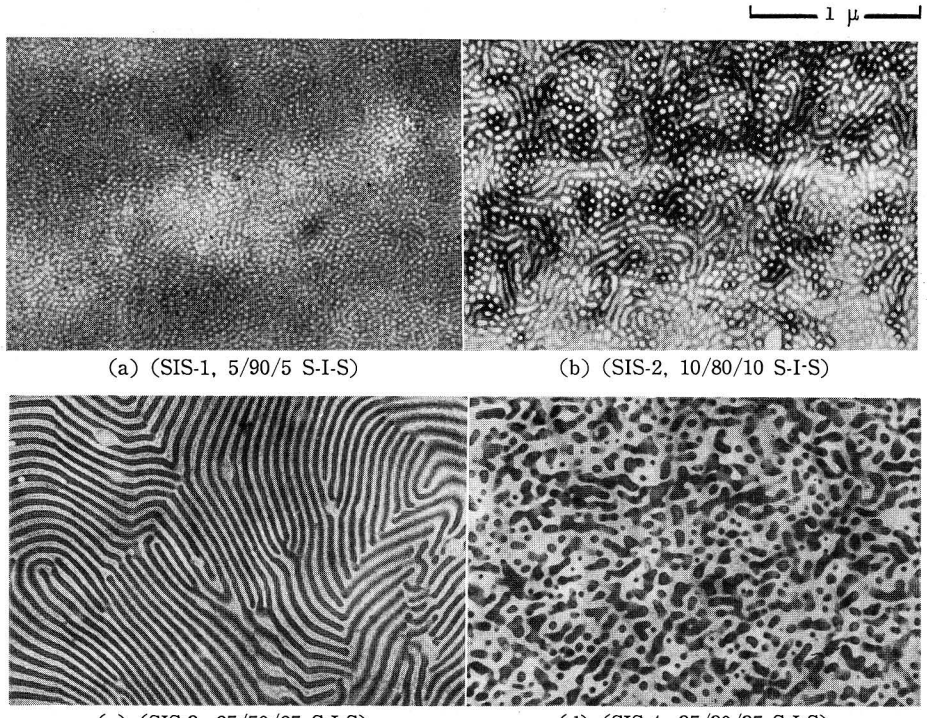

(a) (SIS-1, 5/90/5 S-I-S) (b) (SIS-2, 10/80/10 S-I-S)

(c) (SIS-3, 25/50/25 S-I-S) (d) (SIS-4, 35/30/35 S-I-S)

Fig. 23. Electron micrographs of urtrathin sections about 350 Å thick, cut normal to the surfaces of films cast from 5% toluene solutions of styrene-isoprene-styrene block copolymers varying in composition from 9.5 to 72% weight fraction of styrene.

23 d) may be characterized, like that in the SIS-2 and/or SIS-1, as curved rods and/or spheres of one component in a matrix of the other component, but the roles of the two components are interchanged.

Although any definite domain structure of dispersed rods or spheres of isoprene component in a matrix of styrene component could not be observed, probably because of the lack of copolymers sufficiently rich in styrene component, the entire systematic sequence of domain structures with increasing fractions of component *A* presumably would appear, as in *A-B* block copolymers: *i.e.*, spheres of component *A* dispersed in a matrix of component *B*, rods of *A* dispersed in *B*, the alternating lamellar arrangement of the two components, rods of *B* dispersed in *A*, and spheres of *B* dispersed in *A*.

Change of Domain Structure with Casting Solvent. In order to investigate the effect of casting solvent on the domain structure, the SIS-4 block copolymer was cast from solutions of about 5% concentration in various solvents at 30°C, the same temperature as the above. Electron microscopic textures obtained

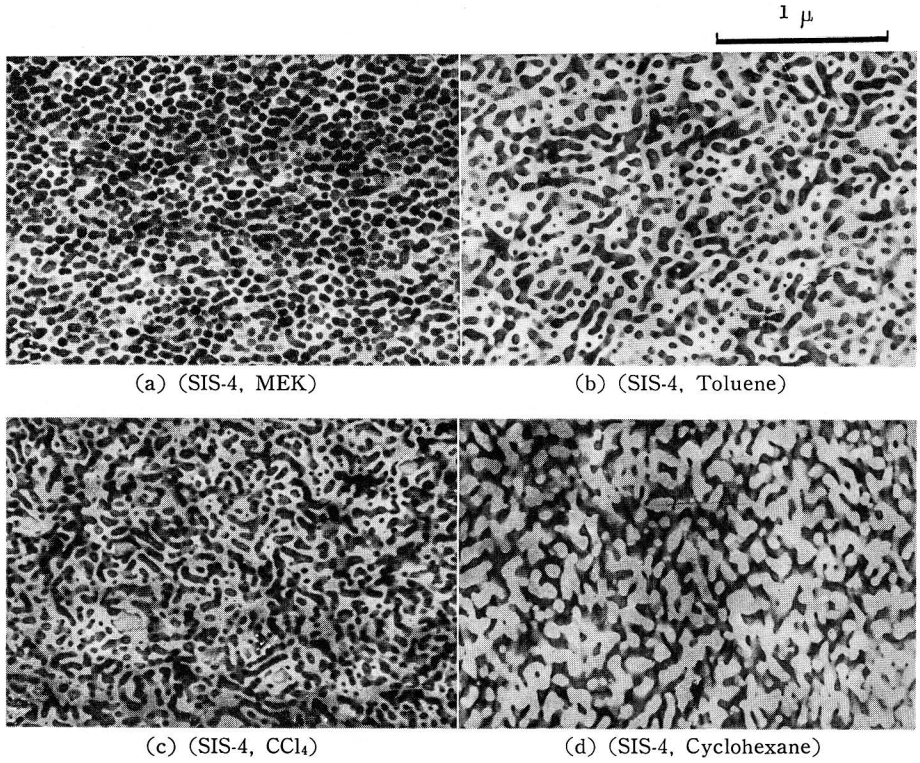

Fig. 24. Electron micrographs of ultrathin sections about 350 Å thick, cut normal to the surfaces of films cast from 5 % solutions of SIS-4 block copolymer in various solvents.

by the technique described earlier are illustrated in Fig. 24.

The domain structures of copolymer SIS-4 cast from methyl ethyl ketone (MEK) (Fig. 24 a), toluene (Fig. 24 b), and carbon tetrachloride (Fig. 24 c) may be classified, in general, as a texture of dispersed spheres or rods of isoprene component in a matrix of styrene component. However, in detail, it may be pointed out that the better the solvent is for polyisoprene, and, in contrast, the poorer the solvent for polystyrene, the isolated spherical domains of isoprene component, as shown in Fig. 24 a, tend to expand more and interconnect to form the rod-like domains, as in Figs. 24 b and 24 c, and, at last, the continuous matrix phase, as seen in Fig. 24 d for cyclohexane in which the styrene component is dispersed, in contrast to the others, as irregular fragments in the matrix of isoprene component.

B. Domain Formation Mechanism and Molecular Arrangements

Related to the appearance of iridescence even in solution, there must be a critical concentration C* at which each block segment of the copolymer

chains undergoes phase separation and aggregates into characteristic molecular micelles.

Fig. 25 shows five possible types of the micelles at the critical concentration C*, such as could organize the five types of the fundamental domain structures by hexagonal close-packing of spherical and rodlike micelles and piling up of lamellar micelles. The two modes of the molecular arrangement within the micelles, *i. e.*, the intermicellar and intramicellar arrangements, are taken into consideration for an *A* sphere in a surrounding *B* shell micelle (Fig. 25 a), an *A* rod in a *B* sheath micelle (Fig. 25 b), and alternating lamellar micelles (Fig. 25 c).

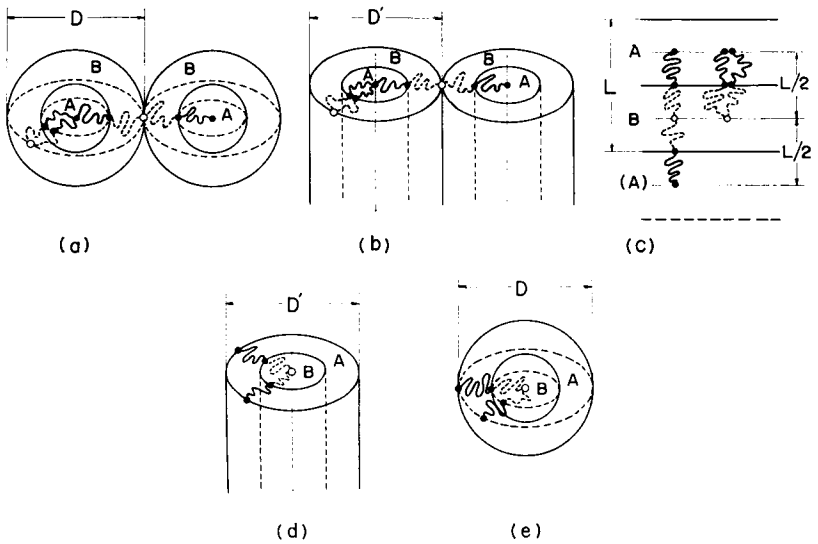

Fig. 25. Schematic representations of five types of micelles and two types of molecular arrangements, intermicellar and intramicellar annangements: (a) A sphere in B shell: (b) A rod in B sheath: (c) alternating lamellae of A and B; (d) B rod in A sheath; (e) B sphere in A shell.

Although the two junction points of the block segments in each copolymer chain must be distributed in the interface between the two phases within the micelles, one of the major difficulties is how to evaluate statistically the perturbations of the block segments within the micelles with differently shaped interfaces that must act as adsorption walls perturbating the configuration of the chain blocks.[50]

As briefly discussed in the previous chapter, Meier treated the problem of the chain perturbations of an *A-B* block copolymer fairly rigorously by solving the diffusion equation for block segments within the spherical domain imposing

the condition of uniform domain density.[42] Recently, he generalized the treatment to the other types of domain structures, *i.e.*, the rodlike and lamellar domains, by introducing a rather ambiguous parameter, taking into account the effects of the perturbations of the block segments in the matrix phase (which were neglected in the former treatment) upon the three types of domain formations.[51] In addition, Leary and Williams[52] have also solved the problem of chain perturbations for the formation of the spherical domain of the *A-B-A* block copolymer by using an approach similar to Meier's, in principle, but more straightfoward, in taking account of the effects of the boundary condition of a pair of spherical domains upon the perturbation of the middle block segments in the matrix phase, where the sphere boundaries were, unfortunately, approximated as two parallel impenetrable planes because of the difficulty of the strict treatment.

The problem, indeed, seems much too complicated to solve exactly by taking strict account of the effects of domain boundaries upon the perturbations of the block segments, and therefore, one has to introduce approximations. One of the crude but simple expedients is to use a common restiction of the molecular arrangements within the respective micelles so that each type of micelle can be discussed to the same order of approximation by use of a relatively simple thermodynamic approach. That is, as was done in the previous chapter for the domain formation of *A-B* block copolymer, some particular points of the block chain may be fixed at some particular positions within the micelles in order to solve the problem of micelle formations as quasi-equilibrium phenomena at the critical micelle concentration in terms of rather simple thermodynamic and molecular parameters.

Let us restrict the position of the center of the middle block at particular points within the micelles, as indicated by the open circles in Fig. 25, in addition to both ends of the block chain and the two junction points of the block segments, as was done in the previous chapter for the *A-B* block copolymer. Thus, for the spherical and rodlike micelles of component *A* in component *B*, the ends of the blocks are at the center of the micelles and the center of the *B* (middle) block is at the point on the outer surface of the respective micelle located on the same radius as the junction point between block segments (Figs. 25 a and 25 b). In the spherical and rodlike micelles of component *B* in component *A*, the roles of the ends of the *A* blocks and the center of the *B* block are reversed (Figs. 25 e and 25 d). For alternating lamellar micelles, the ends of the *A* blocks and the center of the *B* block are at points in the center layer of each lamella lying on a line perpendicular to the inter-

face through the junction point (Fig. 25 c).

Then, when the *A-B-A* block copolymer is treated as twice the *A*-(1/2)*B* block copolymer, the five typers of micelle structures may be interpreted in terms of thermodynamic and molecular parameters by using an approach quite similar to that in the previous chapter. The approximation is, of course, of the same or rather a lower order of approximation than the previous one, in that it neglects the extreme of density fluctuations at the center and outer surface of the micelles, makes no explicit distinction between intermicellar and intramicellar molecular arrangements, and, in addition, underestimates the contribution of the configurational entropy of the middle block to the free energy of the respective micelle formation because of the restiction of the center of the middle block at particular points within the micelles.+

The Gibbs free energy of each type of micelle at the critical micelle concentration C*, the size of the micelle at the minimum free energy, and the minimum free energy itself, can be formulated as functions of molecular parameters much like Eqs. (1) through (4) in the previous chapter just by replacing n_B with $(1/2)n_B$. As was recognized by Eq. (3), the equilibrium size of the respective micelle is given by the product of $f_i(\phi, \sigma, n)$ and $(\Delta W/kTN)^{1/3}$. When one assumes that the micelle is dried up to the corresponding domain while keeping the number of block segments within the micelle unchanged, the size of the respective domain in the dry state may be given by the following equations,[53] depending on whether the micelle shrinks isotropically or anisotropically during drying:

for the spherical domain:

$$D_d{}^3 = f_s{}^{*3} \frac{\Delta W m_A n_A{}^2 a_A{}^2 \sigma_A{}^2}{kT\rho N_0} \tag{7}$$

where f_s* is given by

$$f_s{}^{*3} = \frac{8(1-V_A)^{2/3}}{(1-V_A{}^{1/3})^2 + (1-V_A)^{2/3}}$$

for the rodlike domain:

$$D'_{d,iso}{}^3 = f_r{}^{*3} \frac{\Delta W m_A n_A{}^2 a_A{}^2 \sigma_A{}^2}{kT\rho N_0} \tag{8}$$

where f_r* is given by

+ The problem of underestimating the contribution of the configurational entropy of the middle block may be solved rigorously by calculating the product of the probability density for finding the two ends of each (1/2)*B* block at a given position within the micelle, and then integrating the result over the entire interior to give an additional entropy term.

$$f_r^{*3} \equiv \frac{(16/3)(1-V_A)^{2/3}}{V_A^{1/6}(1-V_A^{1/2})^2+V_A^{1/2}(1-V_A)^{2/3}}$$

$$D'_{d,}{}^2{}_{aniso} = f_r^{**2}(\Delta W/kt)^{2/3}\frac{m_A n_A^{7/6} a_A^{1/3}\sigma_A^{1/2}}{(4\pi/3)^{1/3}(1/6)^{1/2}\rho N_0} \tag{8'}$$

where f_r^{**} is given by

$$f_r^{**3} \equiv \frac{(16/3)(V_A C)^{1/2}(1-V_A)^{2/3}}{V_A^{1/6}(1-V_A^{1/2})^2+V_A^{1/2}(1-V_A)^{2/3}}$$

for the lamellar domain:

$$L^3{}_{d,iso} = f_l^{*3}\frac{\Delta W m_A n_A{}^2 a_A{}^2 \sigma_A{}^2}{kT\rho N_0} \tag{9}$$

where f_l^* is given by

$$f_l^{*3} \equiv f_l^3/n_A a_A{}^2\sigma_A{}^2$$

$$L^3{}_{d,aniso} = f_l^{**3}(\Delta W/kT)(m_A n_A/\rho N_0) \tag{9'}$$

where f_l^{**} is given by

$$f_l^{**3} \equiv \frac{(8/3)V_A{}^2(1-V_A)^{2/3}C^2}{(4\pi/3)^2(1/6)^3[V_A{}^{2/3}(1-V_A)^2+V_A{}^2(1-V_A)^{2/3}]a_A\sigma_A}$$

Here anisotropic shrinking means the micelle shrinking only in a direction perpendicular to its interface, N_0 is Avogadro's number, and C is given by

$$C = N\left[(4\pi/3)<\frac{1}{6}n_A a_A{}^2\sigma_A{}^2>^{3/2}+(4\pi/3)<\frac{1}{6}n_B a_B{}^2\sigma_B{}^2>^{3/2}\right]$$

According to Eqs. (7) through (9), the size of the spherical domain is proportional to the following power of degree of polymerization of the block, *i.e.*, the (2/3)th power for the spherical domain; the (2/3)th through (7/12)th power for the rodlike domain; and the (2/3)th through (1/3)th power for the lamellar domain, depending on the isotropic or anisotropic shrinking of the micelle.

When the *A-B-A* type block copolymer is compared with the *A-B* type block copolymer, both having identical molecular weight and fractional composition of *A* and *B* components, the size of, for example, the lamellar domain for the *A-B-A* block copolymer, $(L_{A,B})_{ABA}$, must be larger than that for the *A-B* block copolymer, $(L_{A,B})_{AB}$, by a factor ranging from $(1/2)^{2/3}$ to $(1/2)^{1/3}$. This situation is demonstrated by comparison in Fig. 26 of the alternating lamellar structure of specimen SIS-3 cast from toluene (Fig. 26 a) with that of an *A-B* block copolymer of styrene and isoprene, SI-2 in Table I, also cast from toluene (Fig. 26 b). Although the molecular weights and the fractional compositions are not exactly identical, the ratio of average size $(\bar{L}_B)_{ABA}$ to $(\bar{L}_B)_{AB}$ is found to be (300Å/450Å), which is fairly close to the value of

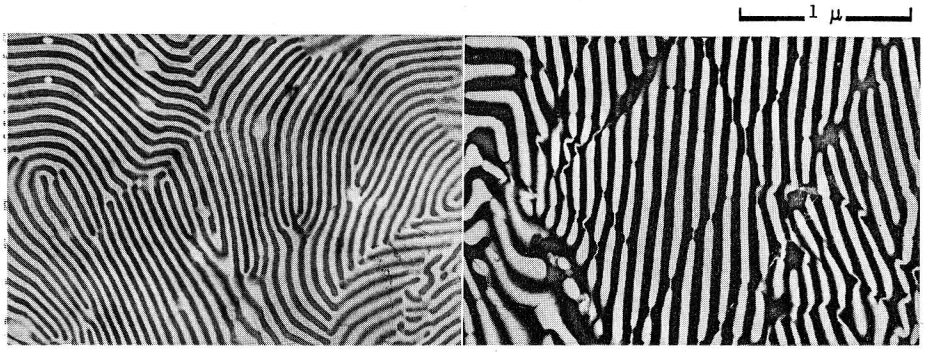

Fig. 26. Comparison of domain size of lamellar structure obtained from A-B-A type block copolymer with that from A-B type block copolymer: (a) cast from a toluene solution of SIS-3; (b) cast from a toluene solution of SI-2, an A-B type block copolymer of same components and almost identical molecular weight and composition as SIS-3.

$(1/2)^{2/3}$.

In addition, Matsuo *et al.*[26] have examined the effects of sequence arrangements of multi-block copolymers of styrene and butadiene upon the domain formation, and concluded that the domain structure is primarily affected by the overall fractional composition of the two components but not by the sequence arrangements, such as *A-B*, *A-B-A*, *B-A-B*, and *A-B-A-B*. The relative size of the rodlike domains of butadiene component obtained from toluene solutions of the *A-B*, *B-A-B*, and *A-B-A* block copolymers, all with the same composition (mole ratio 60/40) of styrene to butadiene, can be explained in terms of the same molecular arrangements as above by treating the *B-A-B* or *A-B-A* block copolymer as twice *B*-(1/2)*A* or *A*-(1/2)*B* block copolymer for their micelle formation. The detail will be discussed elsewhere[53] by gathering the possible data for the domain size that has appeared in the literature.[23,25,26,44]

C. Swelling Behavior of an A-B-A Type Block Copolymer in Relation to Molecular Arrangements

As mentioned in the previous sections, the role of the interdomain arrangement of an *A-B-A* block copolymer in the formation of spherical and rodlike domains of component *A* in component *B*, as well as of alternating lamellar structure, must be reflected in the difference of bulk properties as compared to those of the *A-B* block copolymer.[42,54-57] This situation may be easily demonstrated in terms of swelling experiments using a solvent, such as *iso*-octane, which is a good solvent for isoprene but a nonsolvent for styrene.

Actually, when one dips film specimens cast from toluene solutions of the *A-B-A* block copolymers, SIS-1, SIS-2, and SIS-3, which exhibit structures either with domains of component *A* dispersed in component *B* or with alternating lamellae, the films are considerably swollen but, unlike films of the corresponding *A-B* block copolymers, they never disintegrate.

In order to investigate the swelling behavior quantitatively in a way similar to that proposed by Bishop and Davison,[58] the dimensional change of four kinds of film specimens cast from toluene solutions of binary mixtures of the SIS-2 copolymer with homo-polystyrene (PS-S, $\bar{M}_n$: 3.34×10^4) in different proportions, as well as film specimens of the copolymers, SIS-2 SIS-3, also cast from toluene, was studied by dipping small pieces *ca.* 1 cm × 1 cm × 0.1 mm in *iso*-octane at 25.0°C. Overall volume fractions of styrene component in the four kinds of binary mixtures are listed in Table 4, together with the specimen codes, Mix-1 through Mix-4, and the domain structures are illustrated in Fig. 27 in terms of the electron micrographs obtained also by the OsO_4 fixation technique. As was expected from the previous studies on the domain forma-

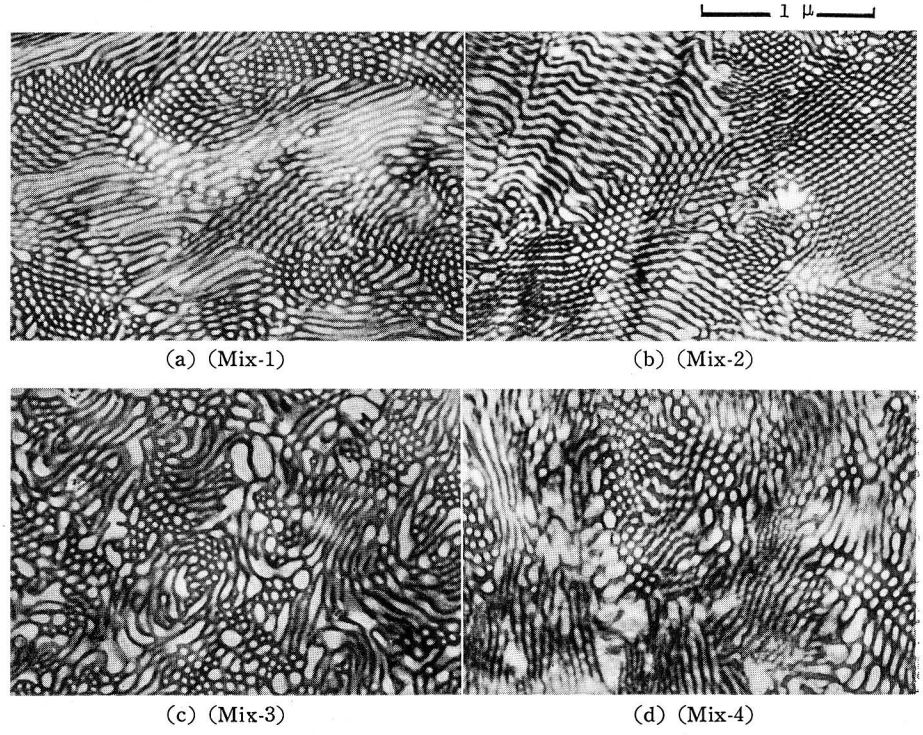

Fig. 27. Electron micrographs of urtrathin sections about 350 Å, cut normal to the surfaces of films cast from 5 % toluene solutions of binary mixtures of SIS-2 copolymer with homo-polystyrene in different compositions.

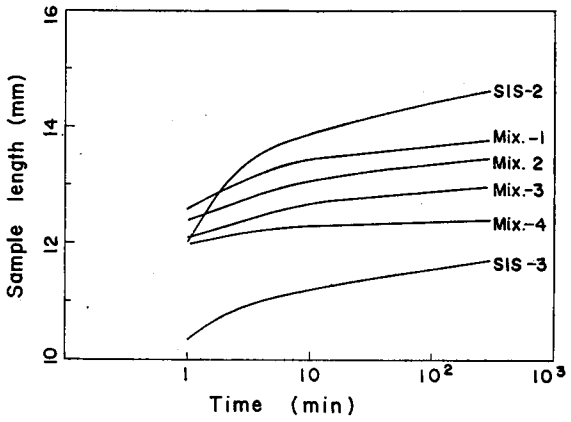

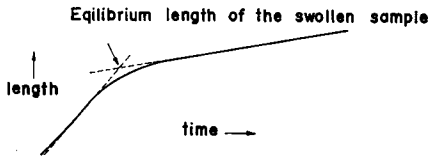

Fig. 28. Swelling behavior of film specimens, cast from toluene solutions of SIS-2 and SIS-3 (Figs. 23 b and 23 c) and four binary mixtures of SIS-2 with homo-polystyrene (Mix-1 through MIX-4) (Figs. 27 a through 27 d), in iso-octane at 25.0°C.

tion in binary or ternary mixtures of *A-B* block copolymers with corresponding homo-polymers, the added homo-polystyrene of relatively lower molecular weight is dissolved in the rodlike domains of styrene blocks of SIS-2 to thicken the rods, as shown in Figs. 27 a through 27 d with increasing amounts of homo-polystyrene.

The swelling behavior of the film specimens is shown in Fig. 28 in terms of the change of specimen length with logarithm of time. As shown in the figure, swelling gives for every specimen a plot against the logarithm of time, exhibiting a smaller slope for long times than for short times. This discontinuous behavior suggests the occurrence of two different swelling mechanisms; one mechanism at shorter times can be ascribed to the swelling of the polyisoprene phase and, subsequently, the other mechanism at longer times, which is partly masked by the first one, may be due to styrene chains and styrene blocks pulling out of the styrene domains. If this is the case, the intersection obtained by extrapolating the two linear portions, as indicated in the

lower half in Fig. 28, may be taken as the equilibrium point of the first mechanism.

Using this intersection as the swelling equilibrium of the polyisoprene phase, the average molecular weight $\bar{M}_c$ of sub-molecule chains between effective cross-linking points may be evaluated from the Flory-Rehner equation ;[59,60]

$$\bar{M}_c = \frac{\rho V (V_r^{1/3} - 2V_r/f)}{\ln(1-V_r) + V_r + \chi V_r^2} \tag{10}$$

Here, ρ is the density of the polyisoprene phase in the swollen state, V is the molar volume of the swelling agent, and χ is the interaction parameter given, for example, by Bristow and Watson as[61]

$$\chi = 0.438 + 0.250\, V_r \tag{11}$$

The functionality of a crosslinking point, which is denoted as f, is taken as 4 in this system, and V_r is the apparent volume fraction of polyisoprene in swollen network given by

$$V_r = \frac{(1-\phi) l_0^3}{(l^3 - l_0^3)} \tag{12}$$

where l_0 and l are the length of the specimen in unswollen and swollen states, respectively, and ϕ is the overall volume fraction of styrene component in the unswollen specimen.

The value of $\bar{M}_c$ thus evaluated for each specimen is listed in column 3 in Table 4. As can be seen from the table, $\bar{M}_c$ is always very small for every specimen with $\bar{M}_n$ of the middle block segment of the copolymer, and, in addition, decreases systematically with increasing overall fractions of styrene component for the series of film specimens of SIS-2, Mix-1 through Mix-4, and SIS-3.

The decrease of $\bar{M}_c$ with increasing ϕ sems to be attributable to the filler effect of the dispersed domains of styrene component in which the middle blocks of isoprene are anchored, and validates evaluation of the true volume

Table 4. Characterization of Films used in Swelling Experiments.

Specimen code	Overall volume fraction of styrene, %	Apparent $\bar{M}_c$	$\bar{M}_n$ of isoprene block, ($\times 10^4$)
SIS-2	20.5	6,300	46.0
Mix-1	25.4	4,800	46.0
Mix-2	28.3	4,000	46.0
Mix-3	31.6	3,400	46.0
Mix-4	35.5	2,700	46.0
SIS-3	43.8	700	24.8

fraction V_{r_0} of polyisoprene in a swollen network by the following Kraus equation :[62]

$$V_{r_0}/V_r = 1-\{3C(1-V_{r_0}^{1/3})+V_{r_0}-1\}\phi/(1-\phi) \tag{13}$$

where C is a constant.

The Kraus equation suggests a linear relation for $1/V_r$ against $\phi/(1-\phi)$. This is realized in Fig. 29 for the series of test specimens including SIS-2 and SIS-3, with a quite good fit, and makes it possible to evaluate V_{r_0} by extrapolating the linear relation to $\phi/(1-\phi)=0$. When one uses the value of V_{r_0}, which is free from the filler effect of the dispersed domains of styrene component, instead of V_r in Eqs. (10) and (11), the value of $\bar{M}_c$ thus corrected is, of course, still very small when compared with $\bar{M}_n$ of the middle block segments of each specimen, and is rather close to the value of 14,000 obtained from the molecular weight dependence of solution viscosities of isoprene homopolymers for the critical molecular weight for formation of the so-called "entanglements" between the molecular chains.[63]

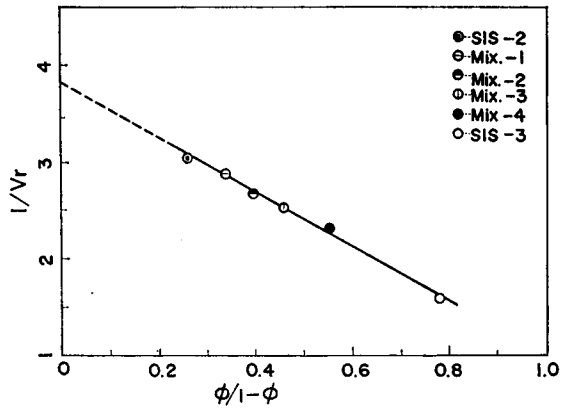

Fig. 29. Linear plot of Kraus equation, $1/V_r$ against $\phi/(1-\phi)$, for evaluating V_{r_0} from the intercept at $\phi/(1-\phi)=0$.

Although Eq. (10) as well as Eq. (13) are primarily based on an isotropic system and the use of the equations for such anisotropic systems having rodlike and lamellar domains oriented roughly parallel to the film surfaces is invalid, it may be qualitatively concluded that the middle block segments of these block copolymers are not only anchored in the dispersed domains to form a coarse network but also entangled with each other to form a fine network within the coarse network. The entanglements between block segments can not be dissolved out even by swelling, because the anchoring of a block

at both ends on the surface(s) of dispersed domains(s), constitutes a sort of permanent crosslink. In other words, the structure may resemble that of carbon-filled rubber vulcanizates.

V. Domain Formation Mechanism of A Graft Copolymer of Poly (Methyl Acrylate) with Styrene from Its Solutions[28]

As mentioned in the introduction of this article, the studies on the domain formation mechanism of graft copolymers have been relatively few in contrast to those for block copolymers. Actually, with the exception of the studies of the POO emulsifying effect of a series of graft copolymers of natural rubber with vinyl monomers by Molau using phase contrast microscopy, most of the studies have speculated on the micelle formation in solutions and the subsequent domain formation in a solid state from their solution and bulk properties, respectively.

In this chapter, the domain structures of a graft copolymer of poly (methyl acrylate) with styrene cast from solutions will be investigated by means of phase-contrast and dye-stained microscopy, and the domain formation mechanism will be discussed in comparison with that of the block copolymer. The result obtained will be useful not only for justifying the speculation of heterogeneous structures of graft copolymer, but also for understanding the more basic problem of the domain formation mechanism of the graft copolymers in terms of some common parameters, especially for highly grafted and multi-block copolymers, irrespective of greatly different molecular structures among the two types of copolymers.

A. Experimental Procedures and Results

1. Preparation of a Graft Copolymer of Poly (methyl acrylate) with Styrene

A series of graft copolymers of poly (methyl acrylate) (PMA) with styrene in different degrees of grafting ranging from 10 to 80 vol % of styrene component, was synthesized by using a coupling technique of living polystyryllithium onto PMA. Methyl acrylate monomer was, first, bulk-polymerized by using α, α'-azobis*iso*-butyronitrile as an initiator (0.005 mole/l), at 50°C for about 3 hrs to keep the polymerization yield less than 3 wt% of the monomer supplied. PMA thus obtained was purified, fractionated, and finally dissolved in THF and sealed in an ampoule equipped with a magnetic breakseal. Polymerization of the styrene monomer was performed in the reaction flask B in Fig. 30 at low temperatures of dryice methanol, to which the sealed THF in flask E was first transferred through the main vacuum line from the flask D, and then the styrene monomer and initiator solution (n-BuLi in heptane) were

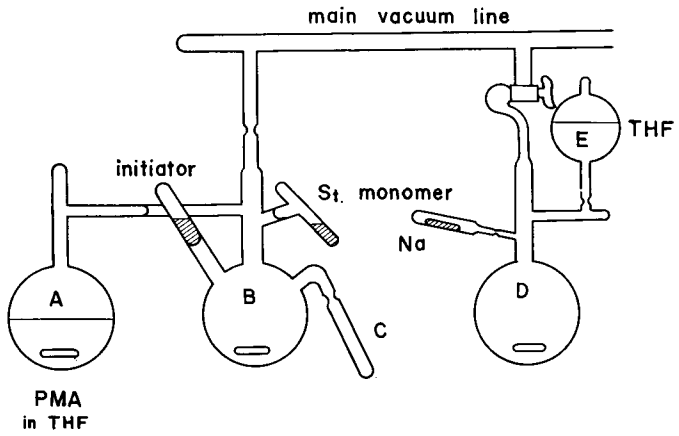

Fig. 30. Schematic representation of graft copolymerization apparatus: (B) reaction flask for anionic polymerization of styrene monomer and graft copolymerization of the living polystyrene onto PMA; (A) flask containing THF solution of fractionated and purified PMA; (C) side-capsule for taking out living polystyrene; (D) purification flask for polymerization solvent; (E) polymerization solvent (THF).

added. The ampoule containing PMA solution in THF, which is designated as flask *A* in Fig. 30, was earlier connected to the flask *B* through its magnetic breakseal, so that the coupling reaction of the living polystyryllithium onto PMA could be performed by moving the PMA solution in THF in the flask *A* to the reaction flask *B* containing the polystyrllithium solution in THF just mentioned. This grafting reaction was also carried out at temperatures of dry-ice methanol for about 30 min until the reddish-yellow color of the living anion of polystyryllithium disappeared completely. The products thus obtained were precipitated by adding methanol to the system.

After drying under vacuum, the precipitate was again dissolved in benzene to make about a 1 % solution, and fractionated by adding *n*-hexane to remove the two homo-polymers from the graft copolymer of PMA with styrene. Fig. 31 shows a typical result of a fractionating curve for one of the precipitates, in which the first fraction, up to about 20 % precipitated, must be the PMA-homo-polymer, the middle fraction, from about 20 to 80 % precipitated, must be the graft copolymer, and the final fraction, up to 100 % precipitated, must be homo-polystyrene. Fig. 32 shows two types of sedimentation patterns of 0.5 g/*l* MEK solutions of the middle fractions by a Spinco Model *E* at 59,780 rpm at 30°C: the lower pattern in Fig. 32 a, a very sharp single peak with a slightly broadened base for a graft copolymer probably well-fractionated; and

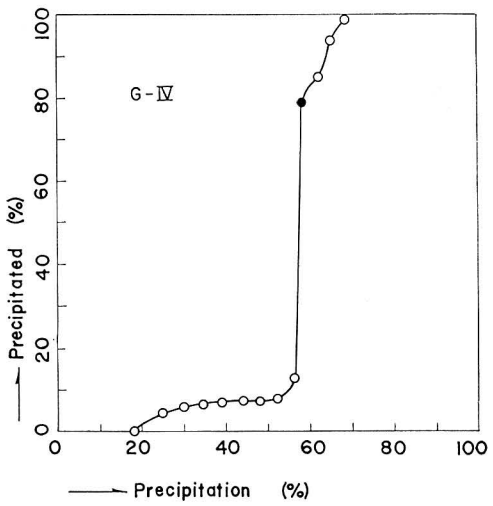

Fig. 31. Typical precipitation behavior of the graft copolymerization product brought about by adding *n*-heptane to a 1 % solution of the product in benzene.

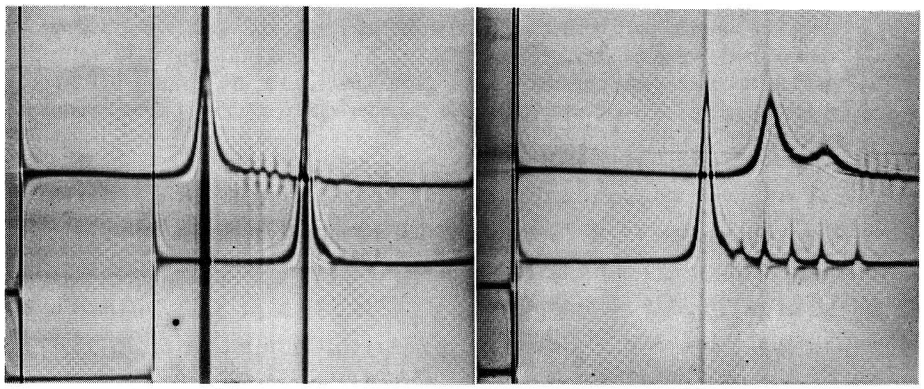

(a) (b)

Fig. 32. Sedimentation pattern from Spince Model E urtracentrifuge: (lower in a) 0.5 g/*l* MEK solution of G-35 graft copolymer of PMA with styrene at 59,780 rpm, (25°C, 18 min; Schlieren angle, 75°); (upper in b) 0.5 g/*l* MEK solution of a graft copolymer of PMA with styrene contaminated with uncoupled PMA at 59,780 rpm, (25°C, 20 min; Schlieren angle, 75°).

the upper pattern in Fig. 32 b, two poorly separated for a graft copolymer poorly fractionated and still contaminated probably with the homo-PMA. Graft copolymers used as test specimens of relatively lower degrees of grafting were selected to have a single peak of sedimentation like the lower pattern in Fig. 32 a by repeating the fractionations, while those of relatively higher degrees of grafting were selected to have a single peak associated with several small peaks like the upper and lower patterns in Figs. 32 a and 32 b, respectively, even after the repeat of the fractionations.

Before the grafting reaction, a part of the polystyryllithium solution in

THF was separated into a side-capsule *C* and taken out by fusing the capsule. The polystyrllithium thus separated, as well as a part of the purified and fractionated PMA already dissolved in THF, were utilized for characterizing the grafted and backbone segments of the graft copolymer, independently. Therefore, it may be noted that this type of graft copolymerization has the advantages of permitting control of the molecular weights and their distributions of the grafted and backbone segments, independently, as well as the grafting density of the grafted segments along the backbone segment, and of having much less probability of crosslinkage between the backbone segments than the other types of graft copolymerizations.

Table 5. Characterization of Graft Copolymer of Poly (methyl acrylate) with Styrene Used,

Specimen code	G-11	G-20	G-35	G-58	G-78
$\bar{M}$ of backborn segment, PMA, ($\times 10^6$)*	3.87	1.32	1.32	3.87	3.87
$\bar{M}$ of grafted segment, PSt, ($\times 10^5$)**	2.09	1.91	1.91	1.38	2.09
Volume fraction of styrene, %	11.0	19.7	34.7	58.4	77.5
No. of grafted segments per backborn segment.	2.2	1.6	4.1	3.66	60.8
Degree of grafting, %+	0.49	1.04	2.66	8.15	13.5
Degree of grafting, α++	0.098	0.198	0.508	1.08	2.70

* Determined from solution viscosity in benzene at 30.0°C by using Basu and Roy's equation.[64]

** Determined from solution viscosity in benzene at 30.0°C by using Krigbaum and Flory's equation.[65]

\+ Defined by the ratio of number of coupling points of polystyryllithium to that of methoxy groups within a backborn segment of PMA.

++ Defined by the value of $(gn_A a_A^2 \sigma_A^2 / n_B a_B^2 \sigma_B^2)$, where g is number of grafted segments per backborn segment and $a_A^2 \sigma_A^2 / a_B^2 \sigma_B^2$ is assumed as unity.

The average molecular weights of the backbone segments, PMA, and the grafted segments, polystyrene, were determined from solution viscosity,[64,65] and listed in Table 5, together with specimen codes of the graft copolymers, which were controlled mostly in the coupling reaction so that the grafting density of polystyryllithium along the backbone segment and, consequently, the volume fraction of the grafted segments varies from about 10 to 80 %. The degree of grafting in Table 5 means the ratio of the number of coupling points to that of the methoxy groups within a backbone segment.

The graft copolymers thus prepared were cast into thin films of about 0.2 mm thick by pouring relatively dilute solutions of about 3 % concentration in benzene onto a glass plate floating on mercury and evaporating the solvent

gradually at about 25°C. The film specimens thus formed were further dried under vacuum for a few days.

2. Domain Structure of the Cast-film from Benzene Solution and the Molecular Arrangement within the Domain.

The domain structure of the film specimen thus prepared was investigated with either a phase-contrast microscope or ordinary microscope using a staining technique with dispersed dyes, such as Miketon Fast Red *R*. That is, thin sections cut into a few microns thickness, normal or parallel to the film surfaces for investigating the domain structure stereo-graphically, were dipped in an aqueous solution of the dispersed dye for about 30 min at temperatures around 40°C. The temperatures are higher than the glass-transition temperature of PMA while still much lower than that of polystyrene so that the dye can easily diffuse into the PMA phase but not into the polystyrene phase, if the two components are separated into the two phases.

Fig. 33 demonstrates the change of domain structure with increasing volume fractions of the grafted segment, where the left-hand side illustrates the phase-contrast micrographs for the thin sections cut normal to the film surfaces of specimens G-11, G-20, and G-35, while the right-hand side illustrates the dye-stained micrographs for those of specimens G-20, G-35, and G-78, both from top to bottom, respectively. As recognized from the comparisons of Fig. 33 b with Fig. 33 b′ for G-20 and of Fig. 30 c with Fig. 30 c′ for G-35, the micrographic patters obtained from the phase-contrast technique begin to resemble those from the dyestained technique less and less as the volume fraction of the grafted segment decreases. This may be due to the much smaller size of the domain compared to the thickness of the thin sections, especially for the specimens, such as G-11 and G-20, having low volume fractions of the grafted segments.

After numerous stereographical observations of the thin sections, the change of domain structures of the film specimens from G-11 through G-78 was concluded to be as follows: G-11 has spherical domains of styrene component, less than 1 micron in diameter, dispersed in a matrix of *MA* component; G-20 has flattened spheroidal domains of styrene component, far less than 1 micron in thickness, oriented in a matrix of *MA* component so that the rotational axis of the flattened spheroid is almost perpendicular to the film surface; G-35 and G-58 have an alternating lamellar structure of the two components, about 1 micron in periodicity, oriented almost parallel to the film surface; and G-78 has spherical domains of *MA* component, up to several

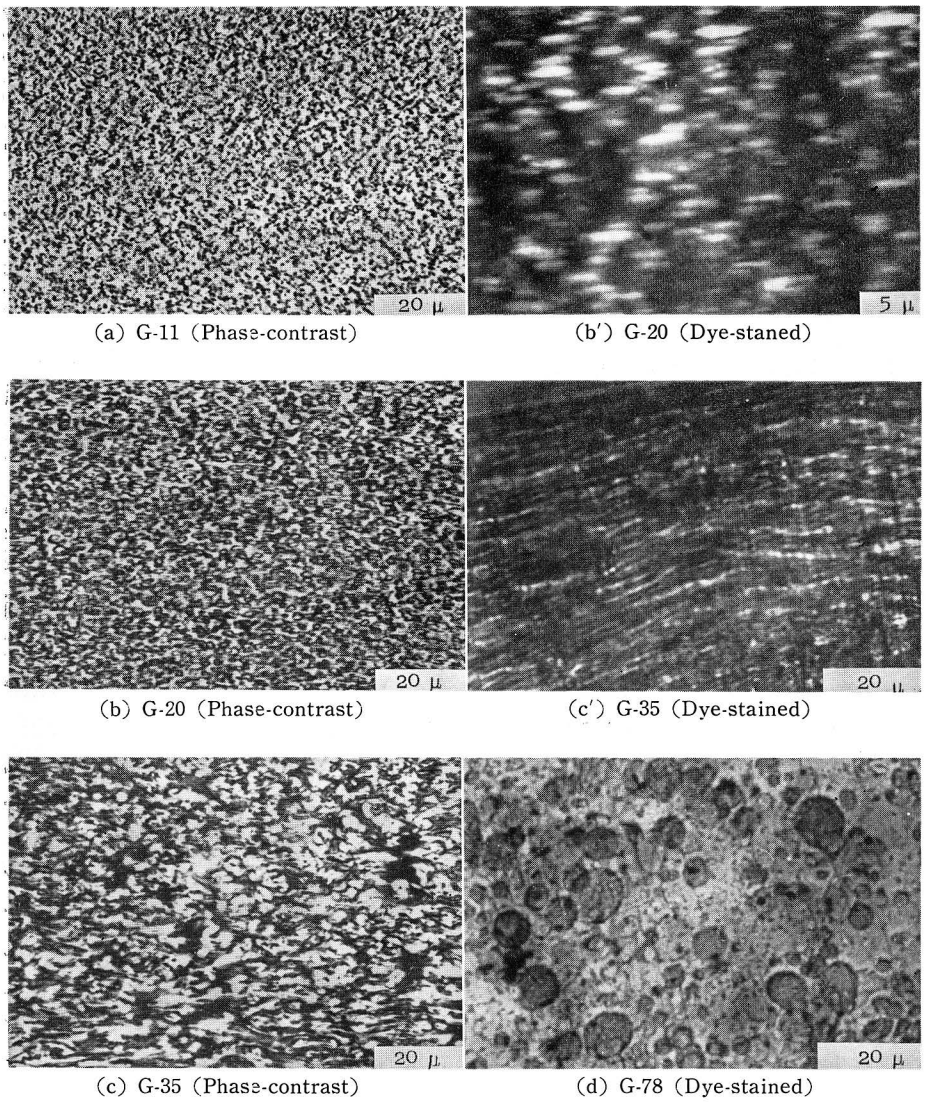

(a) G-11 (Phase-contrast) (b′) G-20 (Dye-staned)

(b) G-20 (Phase-contrast) (c′) G-35 (Dye-stained)

(c) G-35 (Phase-contrast) (d) G-78 (Dye-stained)

Fig. 33. Micrographs of thin sections (a few microns) cut normal to the surfaces of films cast from 3 % benzene solutions of graft copolymers of PMA with styrene varying in the volume fraction of styrene component from about 10 to 80 %: right-hand side, phase-contrast micrographs; left-hand side, dyestained micrographs.

microns in diameter, dispersed in a matrix of styrene component.

When compared with the systematic change of domain structures of the *A-B* and *A-B-A* type block copolymers with an increasing fractional composition of the *A* block segment, *i. e.*, from spherical domains of *A* dispersed in

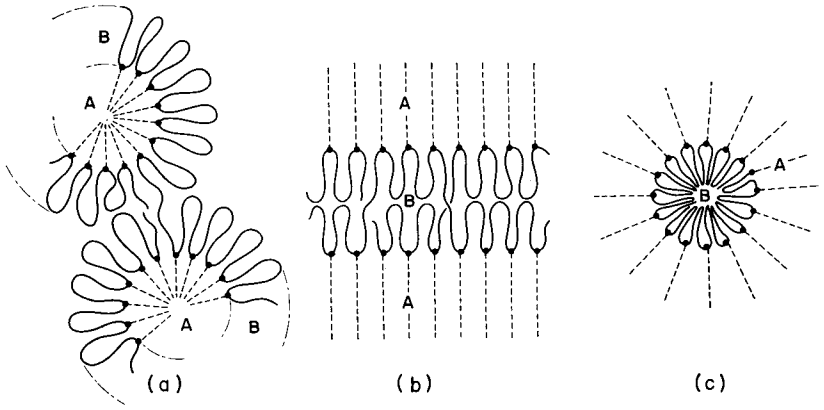

Fig. 34. Schematic representations of three types of domain structures of graft copolymer and two types of molecular arrangements within the domains: (a) spheres of A component (grafted segment) dispersed in a matrix of B component (backbone segment): (b) alternating lamellar arrangement of the two components; and (c) spheres of B component dispersed in a matrix of A component. Intradomain and interdomain arrangements of backbone segments are taken into consideration for (a) and (b), while only the intradomain arrangement of the backbone segment is taken for (c).

a matrix of *B*, to rodlike domains of *A* in a matrix of *B*, to an alternating lamellar structure of the two components, to rodlike domains of *B* in a matrix of *A*, and to spherical domains of *B* in a matrix of *A*, the rodlike domain structures are missed but a flattened spheroidal domain structure is found for the first time.

Fig. 34 shows schematic diagrams of possible molecular arrangements of graft copolymer (backbone segment of component *B* and grafted segment of component *A*) within three types of representative domain structures, *i.e.*, *A* domains in *B* matrix, alternating lamellar structure, and *B* domains in *A* matrix, on the basis of microphase separation of the two kinds of segments forming the domain structures. It is emphasized that two types of molecular arrangements within the domain, *i.e.*, intradomain and interdomain arrangements, may be possible for the domain formation of the former two types of domain structures, but, in contrast, only the intradomain arrangement may be possible for the latter type of domain structure.

B. Domain Formation Mechanism of a Graft Copolymer at a Critical Micelle Concentration

Although the iridescent color effect was not observed so clearly as in the case of the block copolymers, the mechanism of domain formation may be discussed in terms of a quasi-equilibrium phenomenon of micelle formation at

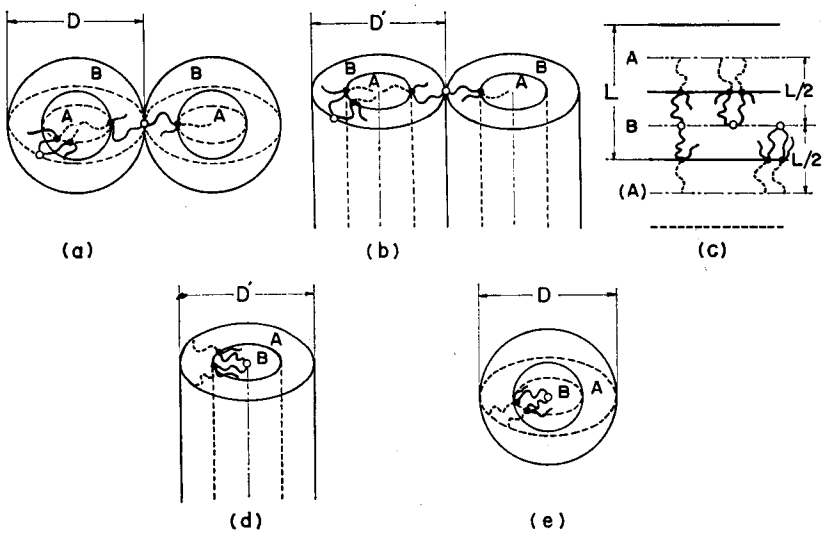

Fig. 35. Schematic representations of five types of micelles of graft copolymers and two types of molecular arrangements within the micelles: (a) and (b): spherical and rodlike micelles of A component (grafted segment) within shell and sheath of B component (backborn segment), respectively; (c) alternating lamellae micelles of the two components; and (e) and (d): spherical and rodlike micelles of B component within shell and sheath of A component, respectively. Intramicellar and intermicellar arrangements of the backbone segment are taken into consideration for (a), (b), and (c), while only the intramicellar arrangement of the backbone segment is taken for (d) and (e).

a critical concentration, resulting from microphase separation of the backbone and grafted segments.

Fig. 35 shows schematic diagrams of micelle structures corresponding to the domain structures in Fig. 34, where two types of rodlike micelles, a *B* rod in an *A* sheath and an *A* rod in a *B* sheath are added. As was done in the previous chapters for the micelle formation of *A-B* and *A-B-A* type block copolymers, when one restricts some particular points of backbone and grafted segments of each graft copolymer at some particular positions within the micelles, the Gibbs free energy of each type of micelle formation may be formulated by using an approach quite similar to those proposed in the previous chapters. That is, for the spherical and rodlike micelles of component *A* (grafted segments) in component *B* (backbone segments), each end of the grafted segments is at the center of the micelles and each middle point of the backbone segment between adjacent graft points is at the point on the outer surface of the respective micelles located on the same radius as one of the adjacent graft points (Figs. 32a and 32b). In the spherical and rodlike

micelles of component B in component A, the roles of each end of the grafted segments and each middle point of the backbone segment between adjacent graft points are reversed (Figs. 32 e and 32 d). For alternating lamellar micelles, each end of the grafted segments and each middle point of the backbone segment are at the middle layers of respective lamellae lying on a line perpendicular to the interface through one of the adjacent graft points. In other words, a graft copolymer is cut at every middle point between adjacent graft points to make T-shaped submolecules, and inlaid in the above fashion into the respective micelles.

Then, five types of micelle structures may be interpreted in terms of thermodynamic and molecular parameters, being of the same order of approximation as that proposed in the previous chapter for the micelle formation of A-B-A block copolymers. This approach is, as was frequently mentioned in the previous chapters, very crude in the sense of absolute evaluation of the free energy of micelle formation, but has the advantage of being commonly used irrespective of the intermicellar and intramicellar arrangements of the backbone segments and may be enough for the relative evaluation of the micelle structures in terms of the parameters.

The micelle size at free energy minimum may be given by[66] (14)

$$D_{G,min}=f_s(\alpha, n_A, a_A, \sigma_A)\cdot\gamma,$$

where f_s is given by

$$f_s\equiv[8V_A^{2/3}n_Aa_A^2\sigma_A^2/\{V_A^{2/3}+4\alpha(1-V_A^{1/3})^2\}]^{1/3} \tag{14'}$$

$$D'_{G,min}=f_r(\alpha, n_A, a_A, \sigma_A)\cdot\gamma, \tag{15}$$

where f_r is given by

$$f_r\equiv[(16/3)V_A^{1/2}n_Aa_A^2\sigma_A^2/\{V_A+4\alpha(1-V_A^{1/2})^2\}]^{1/3} \tag{15'}$$

$$L_{G,min}=f_l(\alpha, n_A, a_A, \sigma_A)\cdot\gamma, \tag{16}$$

where f_l is given by

$$f_l\equiv[(8/3)n_Aa_A^2\sigma_A^2/\{V_A^2+4\alpha(1-V_A)^2\}]^{1/3} \tag{16'}$$

and the free energy minimum itself may be given by

$$G_{s,min}=\{3V_A^{2/3}f_s^{-1}-(3/2\gamma^2)\}3kTN\gamma^2 \tag{17}$$

$$G_{r,min}=\{2V_A^{1/2}f_r^{-1}-(3/2\gamma^2)\}3kTN\gamma^2 \tag{18}$$

$$G_{l,min}=\{f_l^{-1}-(3/2\gamma^2)\}3kTN\gamma^2 \tag{19}$$

where $\gamma^3=\Delta W/kTN$, $\alpha=gn_Aa_A^2\sigma_A^2/n_Ba_B^2\sigma_B^2$, and g is the number of grafted segments per backbone segment.

Comparison of $G_{i,min}$ among the five types of micelles can be made by examining the first term of the right-hand side of Eqs. (17) through (19).

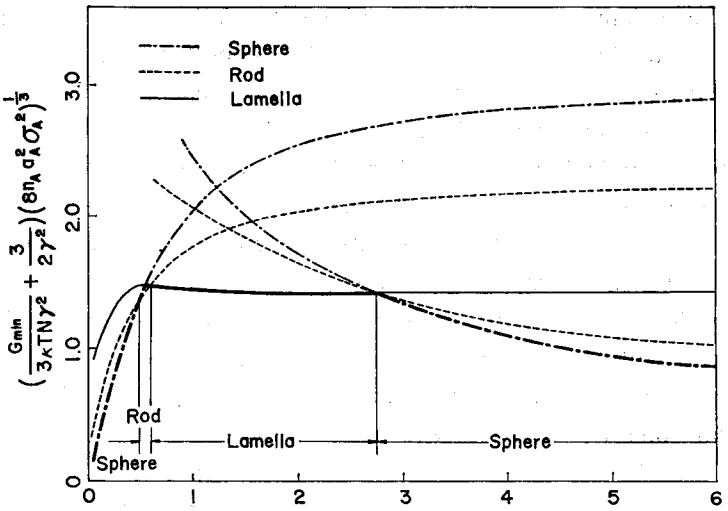

Fig. 36. Relationship between the relative minimum free energy of micelle formation and the parameter α, a sort of degree of grafting, for five types of micelles; A sphere in B shell, A rod in B sheath, alternating lamellae of A and B, B rod in A sheath, and B sphere in A shell.

Fig. 36 shows the above relative values of minimum free energies as a function of α, a sort of degree of grafting in which the numerical values of n_A, n_B, a_A, a_B, and σ_A/σ_B are included.

As seen in Fig. 36, the relative free energy minimum for the rodlike micelles, either of *A* rod in *B* sheath or *B* rod in *A* sheath, can not be at the lowest level at any value of α, except for a narrow interval of α around 0.5. This means that the two types of rodlike micelles, even *A* rod in *B* sheath, are hardly realized, but that the *A* sphere in *B* shell micelle, the alternating lamellar micelle, and the *B* sphere in *A* shell micelle are formed, as indicated by thicker lines in Fig. 36, with increasing values of α. Actually, as demonstrated in the observation of domain structures in Fig. 33 in the previous section, neither of the rodlike domains, *A* rod in *B* matrix or *B* rod in *A* matrix, was found. The flattened sheroidal domain, which was found for the first time for a graft copolymer of G-20, may correspond to an intermediate between the spherical and alternating lamellar micelles having the value of α around 0.5, though the copolymer has a value for α of about 0.2 on the basis of assuming $(a_A^2\sigma_A^2/a_B^2\sigma_B^2)=1$.

Although the relatively large size of domain, up to about 1 micron for the film specimens of G-35 and G-58, both having alternating lamellar structure, may be understood when taking into account the relatively large molecular weights of the backbone segments amounting to a few millions, the huge size

of the spherical domain of the *MA* component, attaining several microns as observed for the film specimen of G-78, is difficult to understand without taking account of either contamination of the graft copolymer with homo-PMA or a localized, not uniformly distributed, coupling reaction of polystyllithum anions onto a particular portion of the backbone segment. The former consideration seems to be minor because of the sedimentation pattern giving a considerably sharp single peak, while the latter one may be realistic for such graft copolymers as G-78, having a high degree of grafting. If this is the case, the molecular weight of the backbone segment within the *T*-shaped submolecules might be practically large enough to make the huge spherical domain.

Strictly speeding, however, the problem of understanding the huge size of the spherical domain found for G-78, must be solved by more definite observation of the domain structure with electron microscopy, using some particular techniques, such as selective burning of one component under electron bombing. On the other hand, it must be kept in mind that the treatment of graft copolymers together with block copolymers is largely speculation which assumes that simple graft copolymers with only a few side chains behave in essentially the same way as block copolymers. This assumption must be the more problematic, when the more complicated the structure of graft copolymer becomes.

IV. Conclusion

In concluding this article, it may be noted that the domain structures of block and simple graft copolymers cast from solutions can be explained in terms of the mechanism of the micelle formation of the copolymers at a critical concentration, being quite analogous to the colloidal behavior of soap molecules at a critical micelle concentration. That is, the microphase separation of homo-polymeric subchains of block and graft copolymers to form particular types of micelles, depends mostly on the overall fractional compositions of the homo-polymeric subchains, not on the sequence arrangements of the block segments and the grafting density of the side chains, and on the interaction between the homo-polymeric subchains for the system in a non-selective solvent and the interactions between the homo-polymeric subchains and solvent for the system in a selective solvent.

For the system of binary or ternary mixtures of the copolymers with homo-polymers corresponding to the subchains, the domain structures cast from their solutions can also be explained in terms of the inherent nature of the micelle formation of the copolymers, just mentioned above, in combination with the solubilization of the homo-polymers into corresponding domanis.

That is, the domain formation mechanism is again quite analogous to the solubilizing effects of a soap micelle and/or the emulsifying effects of soap molecules on the solutes. The problem to be solved is how to correlate quantitatively the binodal surface in the phase diagram of the four component system, the copolymer, corresponding homo-polymers, and solvent, with the critical micelle concentration.

Relating to the bulk properties of a heterogeneous system of two polymer components, it must be emphasized that the properties, especially the mechanical properties,[17,54,67-79] are affected not only by the molecular structures of the components, but greatly by the supermolecular structures of the system, *i.e.*, the textures of the heterogeneous system, which are, indeed, well-controlled by utilizing the mechanism of the domain formations of the block and graft copolymers. In other words, the shape and size of the domain structures, as well as the molecular architectures within the domains, can be controlled in terms of the molecular and thermodynamic parameters of the system, realizing a catchword "Tailor-made Textures with Tailor-made Molecules".

The studies carried out here must be classified as a system of polymeric oil-in-oil emulsions (POO emulsions) in terms of the colloidal behavior of the copolymers. The studies on the systems of polymeric water-in-oil and oil-in-water emulsions (PWO and POW emulsions) must be interesting for developing new composite materials by using hydrophilic and hydrophobic subchains. In addition, the behavior of the block and graft copolymers of crystalline/amorphous and crystalline/crystalline subchains as well as *A-B-C* type block copolymers must be compared with the present work on the copolymers of amorphous/amorphous subchains.

Acknowledgements

The authors are deeply indebted to Drs. K. Kato and Y. Itoh and to Messrs. Y. Yoshimoto and M. Nishimura, Pioneering Research and Development Laboratories, Toray Industries, Inc., for kindly arranging for preparation of the electron micrographs used in this study. A part of this work was supported by a grant from the Scientific Research Funds (Kagaku Kenkyu-hi, 85181-1970) of the Ministry of Education, Japan, and grants from the Japan Synthetic Rubber Co., Ltd., Tokyo, Japan, and the Bridgestone Tire and Rubber Co. Ltd., Tokyo, Japan.

References

1) F. M. Merrett, Trans. Faraday Soc., **50**, 759 (1954).
2) F. M. Merrett, Ric. Sci., **25**, 279 (1955).

3) G. E. Molàu, *Block Polymers*, Aggarwal, ed., pp. 79-106, Plenum Press, New York, 1970.
4) C. Sadron, Angew. Chem., **75**, 472 (1963).
5) B. Gallot, B. Mayer, and C. Sadron, Compt. Rend. Acad. Sci., Paris, **263 C**, 42 (1966).
6) E. Vanzo, J. Polymer Sci., A-1, **4**, 1727 (1966).
7) G. E. Molau, J. Polymer Sci., A, **3**, 1267 (1965).
8) G. E. Molau, J. Polymer Sci., A, **3**, 4235 (1965).
9) G. E. Molau and H. Keskkula, J. Polymer Sci., A-1, **4**, 1595 (1966).
10) G. Riess, J. Kohler, C. Tournut, and A. Banderet, Macromol. Chem., **101**, 58 (1967).
11) J. Kohler, G. Riess, and A. Banderet, European Polymer J., **4**, 173 (1968).
12) Y. Gallot, M. Leng, H. Benoit, and P. Rempp, J. Chim. Phys., **59**, 1093 (1962).
13) Y. Gallot, E. Franta, P. Rempp, and H. Benoit, J. Polymer Sci., C, **4**, 473 (1963).
14) A. Dondos, P. Rempp, and H. Benoit, J. Chim. Phys., **62**, 821 (1965).
15) A. Dondos, P. Rempp, and H. Benoit, J. Polymer Sci., B, **4**, 293 (1966).
16) F. M. Merrett, J. Polymer Sci., **24**, 467 (1957).
17) T. Soen, T. Horino, Y. Ogawa, and H. Kawai, J. Appl. Polymer Sci., **10**, 1499 (1966).
18) K. Kato, Japan Plastic, **19**, No. 10, 89 (1968).
19) C. B. Bucknall, Brit. Plastics, **40**, 118 (1967).
20) M. Szwarc, M. Levy, and R. Milkovich, J. Am. Chem. Soc., **78**, 2656 (1965).
21) S. Schlick and M. Levy, J. Phys. Chem., **64**, 883 (1960).
22) T. Inoue, T. Soen, H. Kawai, M. Fukatsu, and M. Kurata, J. Polymer Science, B, **6**, 75 (1968).
23) T. Inoue, T. Soen, T. Hashimoto, and H. Kawai, J. Polymer Sci., A-2, **7**, 1283 (1969).
24) T. Inoue, T. Soen, T. Hashimoto, and H. Kawai, Macromolecules, **3**, 87, (1970).
25) T. Uchida, T. Soen, T. Inoue, and H. Kawai, J. Polymer Sci., A-2, **10**, 101 (1972).
26) M. Matsuo, S. Sagae, and H. Asai, Polymer (London), **10**, 79 (1969).
27) J. C. Saam and F. W. Gorden Fearon, ACS Polymer Preprints, **11**, 455 (1970).
28) T. Ono, M. S. Thesis presented to the Department of Polymer Chemistry, Faculty of Engineering, Kyoto University, March 11, 1969; presented before the 18 th Annual Meeting of the Society of Polymer Science, Japan, Kyoto, May 20, (1969).
29) K. Kato, Polymer Eng. Sci., **7**, 38 (1967).
30) M. Morton, A. A. Rembaum, and J. L. Hall, J. Polymer Sci., A, **1**, 361 (1963).
31) M. Morton and R. Milkvich, J. Polymer Sci., A, **1**, 443 (1963).
32) M. Morton, E. E. Bostick, and R. G. Clarke, J. Polymer Sci., A, **1**, 475 (1963).
33) A. A. Korotkov, L. A. Shibayev, L. M. Pyrkov, V. G. Aldoshin, and S. I. Frenkel, Vysokomol. Soedin., **1**, No. 3, 443 (1959).
34) K. Fujino, Y. Ogawa, and H. Kawai, J. Appl. Polymer Sci., **8**, 2147 (1964).
35) P. A. Small, J. Appl. Chem., **3**, 71 (1953).
36) R. Zbinden, "Infrared Spectroscopy of High Polymers", Academic Press, New York, 1964.
37) S. Krimm, Fortsch. Hochpolym. Forsch. **2**, 51 (1960).
38) E. F. Gurnee, L. T. Patterson, and R. D. Andrews, J. Appl. Phys., **26**, 1106 (1955).
39) J. F. Rudd and E. F. Gurnee, J. Appl. Phys., **28**, 1096 (1957).
40) A. E. Skoulios, G. Tsouladze, and E. Franta, J. Polymer Sci., C, **4**, 507 (1963).
41) S. Ye. Bresler, L. M. Pyrkov, S. I. Frenkel, L. A. Laius, and S. I. Klenin, Vysokomol. Soedin., **4**, 250 (1962).
42) D. J. Meier, J. Polymer Sci., C, **26**, 81 (1969).
43) T. Soen, T. Uchida, T. Ono, T. Inoue, and H. Kawai, paper presented at the 19 th Annual Meeting of the Society of Polymer Science, Japan, Tokyo, May 23, 1970.
44) E. B. Bradford and E. Vanzo, J. Polymer Sci., A-1 **6**, 1661 (1968).
45) A. Dobry and F. Boyer-Kawenoki, J. Polymer Sci., **2**, 90 (1947).
46) R. S. Scott, J. Chem. Phys., **17**, 279 (1949).

47) E. J. Clayfield and E. C. Lumb, J. Colloid Interfac. Sci., **22**, 269 (1966).
48) D. J. Meier, J. Phys. Chem., **71**, 1861 (1967).
49) P. J. Flory, "Principle of Polymer Chemistry", Cornell Univ. Press, Ithaca, N. Y., 1953.
50) E. A. DiMarzio, J. Chem. Phys., **6**, 2101 (1965).
51) D. J. Meier, ACS Polymer Preprints, **11**, 400 (1970).
52) D. J. Leary and M. C. Williams, J. Polymer Sci., B, **8**, 335 (1970).
53) T. Soen, T. Inoue, K. Miyoshi, and H. Kawai, submitted to J. Polymer Sci., A-2.
54) H. Hendus, K. H. Illers, and E. Ropte, Kolloid-Z., **216-217**, 110 (1967).
55) C. W. Childers and G. Kraus, Rubber Chem. Technol., **40**, 1183 (1967).
56) J. F. Beecher, L. Marker, R. D. Bradford, and S. L. Aggarwal, ACS Polymer Preprints, **8**, 1532 (1967).
57) G. Holden, E. T. Bishop, and N. R. Legge, J. Polymer Sci., C **26**, 37 (1969).
58) E. T. Bishop and S. Davison, J. Polymer Sci., C, **26**, 59 (1969).
59) P. J. Flory and J. Rehner, J. Chem. Phys., **11**, 521 (1943).
60) P. J. Flory, J. Chem. Phys., **18**, 108 (1950).
61) G. M. Bristow and W. F. Watson, Trans. Faraday Soc., **54**, 1567 (1958).
62) G. Kraus, J. Appl. Polymer Sci., **7**, 861 (1963).
63) L. J. Fetters, J. Res. Natl. Bur. Stds., **69 A**, 33 (1965).
64) S. Basu and H. Roy, J. Sci. Ind. Res., **11 B**, 90 (1952).
65) W. R. Krigbaum and P. J. Flory, J. Polymer Sci., **11**, 37 (1953).
66) T. Ono, H. Minamiguchi, T. Soen, and H. Kawai, submitted to Kolloid-Z.
67) R. Zelinski and C. W. Childers, Rubber Chem. Technol., **41**, 161 (1968).
68) M. Morton, J. E. MaCrath, and P. C. Juliano, J. Polymer Sci., C, **26**, 99 (1969).
69) J. F. Beecher, L. Marker, R. D. Bradford, and S. L. Aggarwal, J. Polymer Sci., C, **26**, 117 (1969).
70) E. Fischer and J. F. Henderson, J. Polymer Sci., C, **26**, 149 (1969).
71) A. A. Rembaum, F. R. Ells, R. C. Morrow, and A. V. Tobolsky, J. Polymer Sci., **61**, 155 (1962).
72) A. V. Tobolsky and A. Rembaum, J. Appl. Polymer Sci., **8**, 307 (1964).
73) M. Bear, J. Polymer Sci., A, **2**, 417 (1964).
74) R. J. Angelo, R. M. Ikeda, and M. L. Wallach, Polymer, **4**, 141 (1965).
75) S. L. Cooper and A. V. Tobolsky, J. Appl. Polymer Sci., **11**, 1361 (1967).
76) C. W. Childers and J. T. Gruver, J. Appl. Polymer Sci., **11**, 2121 (1967).
77) C. W. Childers and J. T. Gruver, Rubber Chem. Technol., **40**, 1153 (1967).
78) M. Matsuo, T. Ueno, H. Hrrino, H. Chujo, and H. Asai, Polymer, **9**, 415 (1968).
79) T. Inoue, M. Moritani, T. Hashimoto, and H. Kawai, Macromolecules, **4**, 500 (1971).